β1-Integrin Deletion From the Lens Activates Cellular Stress Responses Leading to Apoptosis and Fibrosis

Yichen Wang, Anne M. Terrell, Brittany A. Riggio, Deepti Anand, Salil A. Lachke, and Melinda K. Duncan

Department of Biological Sciences, University of Delaware, Newark, Delaware, United States

PURPOSE. Previous research showed that the absence of β1-integrin from the mouse lens after embryonic day (E) 13.5 (β1MLR10) leads to the perinatal apoptosis of lens epithelial cells (LECs) resulting in severe microphthalmia. This study focuses on elucidating the molecular connections between β1-integrin deletion and this phenotype.

METHODS. RNA sequencing was performed to identify differentially regulated genes (DRGs) in β1MLR10 lenses at E15.5. By using bioinformatics analysis and literature searching, Egr1 (early growth response 1) was selected for further study. The activation status of certain signaling pathways (focal adhesion kinase [FAK]/Erk, TGF-β, and Akt signaling) was studied via Western blot and immunohistochemistry. Mice lacking both β1-integrin and Egr1 genes from the lenses were created (β1MLR10/Egr1−/−) to study their relationship.

RESULTS. RNA sequencing identified 120 DRGs that include candidates involved in the cellular stress response, fibrosis, and/or apoptosis. Egr1 was investigated in detail, as it mediates cellular stress responses in various cell types, and is recognized as an upstream regulator of numerous other β1MLR10 lens DRGs. In β1MLR10 mice, Egr1 levels are elevated shortly after β1-integrin loss from the lens. Further, pErk1/2 and pAkt are elevated in β1MLR10 LECs, thus providing the potential signaling mechanism that causes Egr1 upregulation in the mutant. Indeed, deletion of Egr1 from β1MLR10 lenses partially rescues the microphthalmia phenotype.

CONCLUSIONS. β1-integrin regulates the appropriate levels of Erk1/2 and Akt phosphorylation in LECs, whereas its deficiency results in the overexpression of Egr1, culminating in reduced cell survival. These findings provide insight into the molecular mechanism underlying the microphthalmia observed in β1MLR10 mice.

Keywords: cell stress, lens, development

The ocular lens is transparent tissue composed of two polarized cell types, lens epithelial cells (LECs) and elongated fiber cells,[1,2] whose basal tips interact with the lens capsule, a thickened basement membrane that completely surrounds the lens.[3] Cell-cell and cell-capsule adhesion and communication are important for lens structural integrity, cellular communication, cell survival, and ultimately, lens transparency.[4–6] The lens expresses a wide variety of cell adhesion molecules that can regulate lens structure and physiology,[7–9] although their functional complexity is generally not well understood.

Integrins are heterodimeric transmembrane adhesion molecules that consist of noncovalently associated α and β subunits.[10,11] They are best known as mediators of bidirectional cell communication with the extracellular matrix and cell surface proteins on neighboring cells.[10,12] The ocular lens expresses β1-integrins in all cells,[13–15] and these proteins are proposed to be major regulators of lens cell contact with their basement membrane (the lens capsule) due to their localization at the basal surface of all lens cells.[16–18] This is consistent with the significant transcript-level expression, in the embryonic day (E)15.5 mouse lens, of several α-integrins that are capable of forming extracellular matrix–binding αβ1 heterodimers. These

include the laminin-binding α6- (19 reads per kilobase per million [RPKM]), the fibronectin/vitronectin/osteopontin binding αV- (8 RPKM), the laminin-binding α3- (5.8 RPKM), the collagen-binding α2- (2.3 RPKM), and the fibronectin binding α5-integrin (2.0 RPKM).[19] Of these, α6β1 and α3β1 are likely to be the functionally most crucial in the lens, as α6/α3-integrin double-null lenses exhibit abnormalities similar to those arising from β1-integrin deletion from the early lens.[15,20] However, no one α-integrin is likely responsible for all lens integrin functions, as suggested by the findings that α6-integrin null lenses exhibit only mild defects,[20,21] whereas α3-integrin[20] and αV-integrin null[22] lenses are morphologically indistinguishable from wild type (WT). Lens integrins also likely regulate growth factor signaling by diverse mechanisms, such as the activation of latent growth factors[22] or direct binding to growth factor receptors in *cis*,[15,23,24] as well as indirectly via integrin-mediated signal transduction.[17,25]

Conditional deletion of β1-integrin from the lens at different stages of development results in distinct phenotypes. For example, removal of β1-integrin from elongating lens fiber cells (using MLR39-Cre) results in a reduction in F-actin localization at fiber cell membranes and altered gap junctional coupling, leading to defects in lens fiber cell structure.[14] In contrast,

TABLE 1. List of All Primers Used for PCR and qRT-PCR

Gene	Sequence of the Primers	Notes
β1-integrin	Fwd: 5′–CGG CTC AAA GCA GAG TGT CAG TC–3′	Recommended by the Jackson Laboratory
	Rev: 5′–CCA CAA CTT TCC CAG TTA GCT CTC–3′	
MLR10-Cre	Fwd: 5′–GCA TTC CAG CTG CTG ACG GT–3′	
	Rev: 5′–CAG CCC GGA CCG ACG ATG AAG–3′	Ref. 94
Egr1	Common Fwd: 5′–GGG CAC AGG GGA TGG GAA TG–3′	Recommended by the Jackson Laboratory
	Rev for WT: 5′–AAC CGG CCC AGC AAG ACA CC–3′	
	Rev for mutant: 5′–CTC GTG CTT TAC GGT ATC GC–3′	
Egr1 (qRT-PCR)	Fwd: 5′–GCA AGT ACC CCA ACC GGC CC–3′	Designed by A. Terrell
	Rev: 5′–CGG CGA TCG CAG GAC TCG AC–3′	
Nab2	Fwd: 5′–GAGGAGGGGTTGCTGGACCG–3′	Ref. 95
	Rev: 5′–GGCTGGAGGCAAAGTCCG–3′	
αSMA	Fwd: 5′–CCGAGATCTCACCGACTACCT–3′	Designed by M. Fisher
	Rev: 5′–GCACAGCTTCTCCTTGATGTG–3′	
Mt1	Fwd: 5′–GCTGTCCTCTAAGCGTCACC–3′	Ref. 96
	Rev: 5′–AGGAGCAGCAGCTCTTCTTG–3′	Ref. 97
Anxa2	Fwd: 5′–ACCAACTTCGATGCTGAGAG–3′	
	Rev: 5′–GCTCCTTTTTGGTCCTTCTC–3′	Designed by A. Terrell
Plat	Fwd: 5′–TACAGAGCGACCTGCAGAGA–3′	
	Rev: 5′–AATACAGGGCCTGCTGACAC–3′	
Mmp14	RT² qPCR Primer Assay for Mouse Mmp14	Qiagen, PPM03617D
Thbs1	Fwd: 5′–CACCTCTCCGGGTTACTGAG–3′	Ref. 98
	Rev: 5′–GCAACAGGAACAGGACACCTA–3′	
Stmn1	Fwd: 5′–GTTCGACATGGCATCTTCTGAT–3′	Ref. 99
	Rev: 5′–CTCAAAAGCCTGGCCTGAA–3′	
Rpl29	Fwd: 5′–TCCGATGACATCCGTGACTA–3′	Ref. 100
	Rev: 5′–TGCATCTTCTTCAGGCCTTT–3′	

Fwd, forward; Rev, reverse.

deletion of *β1-integrin* earlier, in the lens vesicle (mouse E10.5) using LE-Cre (β1LE), results in the exit of LECs from the cell cycle, activation of ectopic Erk and bone morphogenetic protein (BMP) signaling, and inappropriate differentiation of the entire lens epithelium into lens fibers.[15] Furthermore, deletion of *β1-integrin* from all lens cells at mouse E12.5 to E13.5 via MLR10-Cre (β1MLR10) leads to disorganization of the lens epithelium with upregulation of α-smooth muscle actin (αSMA) expression by E16.5, and extensive apoptosis of LECs by birth, resulting in the absence of lenses in adults.[26] However, the molecular basis of β1-integrin function in the lens and the reasons underlying differences between the β1LE and β1MLR10 lens phenotype remain unclear.

In this study, the molecular phenotype of β1MLR10 lenses was characterized by RNA-sequencing (RNA-seq)–based transcriptome analysis. We find that β1-integrin deletion results in the elevated expression of a cohort of genes associated with the cellular stress response, as well as those involved in epithelial to mesenchymal transition (EMT), including several immediate early response transcription factors, most notably early growth response 1 (Egr1). Further, we find that deletion of *Egr1* in β1MLR10 mice partially rescues the ocular defects. Thus, these findings serve to highlight how upregulation of a single factor, Egr1, contributes to the ocular phenotype in β1MLR10 mice and provides new insights into the function of β1-integrins in the ocular lens.

METHODS

Animals

All animal experiments described in this article conform to the ARVO Statement for the Use of Animals in Ophthalmic and Vision Research. Mice were maintained and bred under specific pathogen-free conditions at the University of Delaware

animal facility. Mice lacking β1-integrin expression in all lens cells via Cre-mediated conditional deletion driven by MLR10-Cre (β1MLR10) or Le-Cre (β1LE) were created as previously described.[15,26] *Egr1* null mice (B6N;129-*Egr1^(tm1Jmi)*/J), in which the *Egr1* gene was disrupted by insertion of a PGK-neo cassette into a coding exon upstream of the DNA-binding domain,[27] were obtained from the Jackson Laboratory (Bar Harbor, ME, USA). *Egr1^−/−* mice were bred to β1MLR10 mice, to create mice carrying the *MLR10-Cre* allele and homozygous for both *β1-integrin* and *Egr1* alleles (β1MLR10/Egr1^−/−). All phenotypic comparisons were done among littermates. No phenotypic differences were found between β1MLR10 and β1MLR10/Egr1^+/+ or β1MLR10/Egr1^+/− mice. All mice carrying β1MLR10 also carry *CP49* mutations due to their genetic background. Noon of the day that a vaginal plug was detected in female mice was considered as E0.5.

DNA Extraction and Genotyping

DNA was isolated from tail snips or embryos using the PureGene Tissue and Mouse Tail kit (Gentra Systems, Minneapolis, MN, USA). Mice were genotyped by PCR using primers described in Table 1.

RNA Sequencing

RNA-seq, data analysis, and filtering were performed as previously described.[19,28,29] Briefly, RNA was isolated from E15.5 β1MLR10 lenses (three biological replicates, 30 lenses per replicate) and E15.5 C57Bl/6<har> lenses (WT; three biological replicates, 75 lenses per replicate), and sequencing libraries produced using the Illumina TruSeq RNA Sample Preparation Kit v2 (Illumina, Madison, WI, USA). The resulting cDNA library was sequenced at the University of Delaware, Delaware Biotechnology Institute, Genotyping and Sequencing Center on an Illumina HiSeq 2000 (Illumina). Bioinformatic
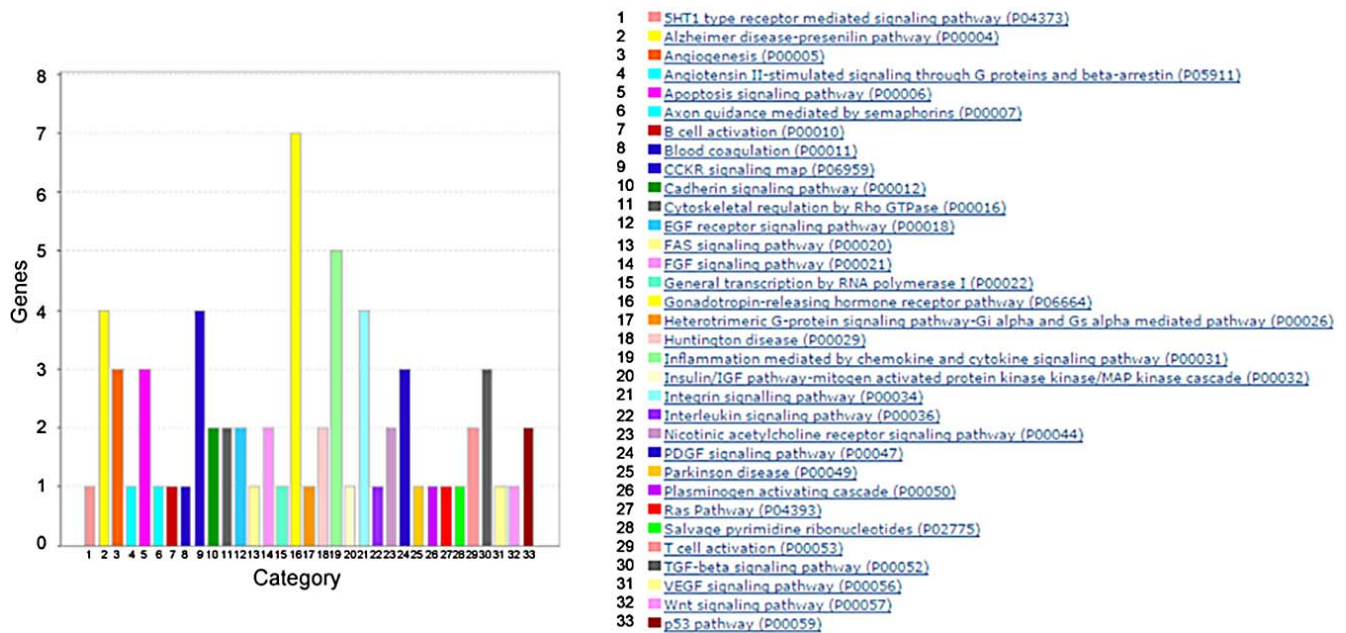
1 5HT1 type receptor mediated signaling pathway (P04373)
2 Alzheimer disease-presenilin pathway (P00004)
3 Angiogenesis (P00005)
4 Angiotensin II-stimulated signaling through G proteins and beta-arrestin (P05911)
5 Apoptosis signaling pathway (P00006)
6 Axon guidance mediated by semaphorins (P00007)
7 B cell activation (P00010)
8 Blood coagulation (P00011)
9 CCKR signaling map (P06959)
10 Cadherin signaling pathway (P00012)
11 Cytoskeletal regulation by Rho GTPase (P00016)
12 EGF receptor signaling pathway (P00018)
13 FAS signaling pathway (P00020)
14 FGF signaling pathway (P00021)
15 General transcription by RNA polymerase I (P00022)
16 Gonadotropin-releasing hormone receptor pathway (P06664)
17 Heterotrimeric G-protein signaling pathway-Gi alpha and Gs alpha mediated pathway (P00026)
18 Huntington disease (P00029)
19 Inflammation mediated by chemokine and cytokine signaling pathway (P00031)
20 Insulin/IGF pathway-mitogen activated protein kinase kinase/MAP kinase cascade (P00032)
21 Integrin signalling pathway (P00034)
22 Interleukin signaling pathway (P00036)
23 Nicotinic acetylcholine receptor signaling pathway (P00044)
24 PDGF signaling pathway (P00047)
25 Parkinson disease (P00049)
26 Plasminogen activating cascade (P00050)
27 Ras Pathway (P04393)
28 Salvage pyrimidine ribonucleotides (P02775)
29 T cell activation (P00053)
30 TGF-beta signaling pathway (P00052)
31 VEGF signaling pathway (P00056)
32 Wnt signaling pathway (P00057)
33 p53 pathway (P00059)

FIGURE 1. PANTHER gene ontology-based pathway analysis (http://pantherdb.org/) of 120 genes differentially regulated in β1MLR10 lenses compared with WT at E15.5. The *bar chart* shows the 33 most represented pathways in which that 120 DRGs were predicted to participate. The number of genes involved in each pathway ranged from one to seven, and most of them included just one to two genes. The top five pathways shown were gonadotropin-releasing hormone receptor pathway (seven genes: Fos, Nab2, Nab1, Ptgfr, Egr1, Mmp14, Junb), inflammation mediated by chemokine and cytokine signaling pathway (five genes: Alox12, Acta2, Pak1, Col6a3, Junb), Alzheimer disease–presenilin pathway (four genes: Mmp2, Acta2, Erbb4, Mmp14), integrin signaling pathway (four genes: Acta2, Itgb8, Col6a3, Col26a1), and CCKR signaling (four genes: Fos, Arhgap4, Pak1, Egr1).

analysis of the resulting data and filtering for significant changes was performed as previously described,[19,28] except that statistical analysis was done using the pairwise quintile-adjusted conditional maximum likelihood method exact test with a Benjamini Hochberg false discovery rate correction run on the EdgeR BioConductor package (http://bioconductor.org).

RNA Isolation/cDNA Synthesis/Quantitative RT-PCR

RNA was isolated from pooled lenses at different embryonic stages (E13.5, E14.5, E15.5, and E16.5; at least three biological replicates derived from independent tissue pools per stage) using the SV Total RNA Isolation System (Promega, Fitchburg, WI, USA). At E15.5, different RNA samples were used for RNA-seq and RT-PCR validations. The RT^2 First Strand Synthesis Kit (Qiagen, Valencia, CA, USA) was used to synthesize cDNA, and this was used in quantitative RT-PCR (qRT-PCR) reactions performed with a QuantiTect SYBR Green PCR Kit (Qiagen) on an Applied Biosystems 7300 Real Time PCR system (Applied Biosystems, Foster City, CA, USA). See Table 1 for primer sequences used in qRT-PCR. Fold change was calculated via the $2^{-\Delta\Delta CT}$ method, and statistical significance was determined by 2-level nested ANOVA.

Bioinformatics Analyses

The filtered differentially regulated gene (DRG) list was analyzed for enriched pathways using PANTHER (Protein ANalysis THrough Evolutionary Relationships, http://www.pantherdb.org/)[30] and analyzed for enriched expression during normal lens development using *iSyTE* (Integrated Systems Tool for Eye Gene Discovery, http://bioinformatics.udel.edu/research/isyte/)[31] as previously described.[28,29] Motif enrichment

analysis was performed on the putative regulatory regions surrounding the transcriptional start site (TSS) of the β1MLR10 lens DRGs ($n = 120$). First, we implemented the iRegulon package[32] (https://omictools.com/iregulon-tool) to identify enrichment of overrepresented transcription factor (TF) binding motifs using the open-access databases for transcription factor binding profiles (Supplementary Table S3). The 10-kb (TSS −5 kb and TSS +5 kb) a priori defined regulatory region (described in Ref. 32) of all 120 DRGs was searched for TF-binding motifs at a significant cutoff of normalized enrichment score (NES) ≥3. Next, Egr1 binding sites similar to the position weight matrix for the Egr1 motif[33] were identified in the region 2.5 kb upstream of the TSS of β1MLR10 lens DRGs ($n = 120$) using an *in-house* script implemented in the *MotifDb* R-package (www.bioconductor.org). This Egr1 motif matching was performed with a minimum score match percentage (80%) using the *matchPMW* function in the "Biostring" package (www.bioconductor.org). The Egr1 logo used in this analysis is shown in Figure 6.

Gross Morphology

Adult mice (age range from 2 to 5 months old) were killed and photographed. Eye tissues were enucleated and photographed using a Zeiss Stemi SV 11 Apo Stereo dissecting microscope (Zeiss, Thornwood, NY, USA) under dark-field illumination. Afterward, lenses were dissected and placed into prewarmed culture Medium 199 (Cellgro; Mediatech, Inc., Manassas, VA, USA) and photographed under bright-field illumination. A minimum of three biological replicates were analyzed for each genotype.

Western Blot (WB)

Protein was extracted from lenses using lysis buffer (50 mM Tris-HCl pH 8.0, 150 mM NaCl, 1% NP-40, 0.5% Na-
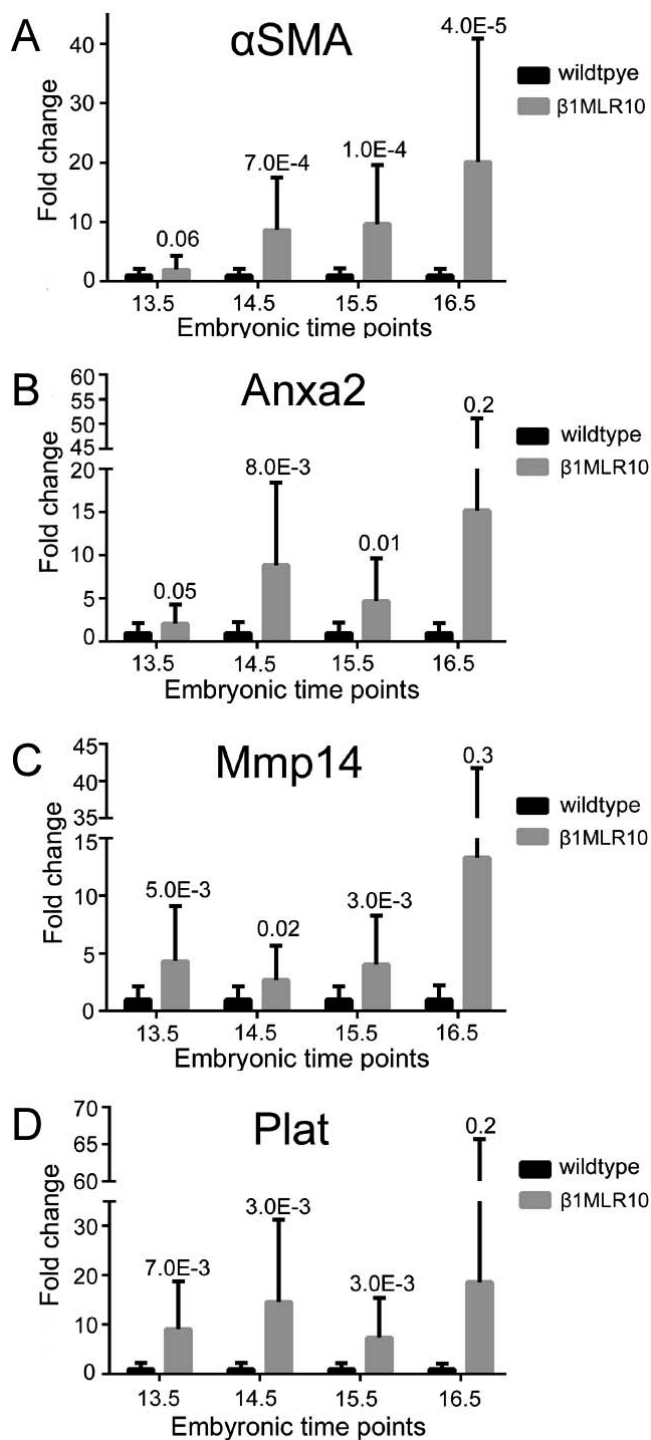
FIGURE 2. qRT-PCR analysis of **(A)** *αSMA*, **(B)** *Anxa2*, **(C)** *Mmp14* (Matrix metalloprotease 14/membrane type I matrix metalloproteinase), and **(D)** *Plat* mRNA expression in WT and β1MLR10 lenses from E13.5 to E16.5. **(A)** Compared with WT, the expression of *αSMA* was significantly higher in β1MLR10 lenses from E14.5 to E16.5. **(B)** Compared with WT, the expression of *Anxa2* was significantly higher in β1MLR10 lenses from E13.5 to E15.5. The elevation in *Anxa2* mRNA at E16.5 was not significant due to the high SD of the data. **(C)** Compared with WT, the expression of *MMP14* was significantly higher in β1MLR10 lenses from E13.5 to E15.5. The elevation in *MMP14* mRNA at E16.5 was not statistically significant due to the high SD of the data. **(D)** Compared with WT, the expression of *Plat* was significantly higher in β1MLR10 lenses from E13.5 to E15.5. The elevation in *Plat* mRNA at E16.5 was not significant due to the high SD of the data. *Error bars* represent SD. Statistical significance was determined with nested ANOVA and is given above the *error bar* in the figure.

deoxycholate, 0.1% SDS) with 1X Halt Protease and Phosphatase Inhibitor Cocktail (Thermo Scientific, Rockford, IL, USA). Protein was loaded and resolved on a 4% to 15% Mini-PROTEAN TGX Precast Gel (Bio-Rad, Hercules, CA, USA) and transferred onto a nitrocellulose membrane (Bio-Rad), followed by blocking and incubation with primary antibodies (see Table 2 for details). The membrane was washed and incubated with horseradish peroxidase conjugated secondary antibody (Calbiochem, San Diego, CA, USA). The membrane was treated with a chemiluminescence detection kit (Amersham Biosciences, Piscataway, NY, USA), and a FluorChem Q SA imager (ProteinSimple, San Jose, CA, USA) was used for imaging and digital quantification. At least three independent biological replicates were analyzed for each antibody and statistical significance was determined by 1-tailed *t*-test.

Immunofluorescence Staining and Confocal Imaging

All immunofluorescence (IF) analyses were performed as previously described.[34] Briefly, embryonic head tissue was collected, while eyes were collected from newborn or adult mice. Tissues were embedded directly in Optimum Cutting Temperature (Tissue Tek, Torrance, CA, USA) and stored at −80°C until 16-μm-thick sections were obtained with a Leica CM3050 cryostat (Leica Microsystems, Buffalo Grove, IL, USA), and mounted on slides (ColorFrost Plus; Fisher Scientific, Hampton, NH, USA). Slides were fixed with either 1:1 acetone-methanol for 20 minutes at −20°C or into 4% paraformaldehyde for 30 minutes at room temperature. Blocking buffer was made in 1X PBS or 1X Tris-buffered saline (TBS), and slides were blocked for 1 hour at room temperature. Sections were then incubated with primary antibody diluted with blocking buffer (see Table 2 for antibodies and dilution rates used) for 1 hour at room temperature, or overnight at 4°C. Slides were then washed in 1X PBS or 1X TBS, and incubated with a solution consisting of Alexa Fluor 488/568 labeled secondary antibody (1:200 dilution; Invitrogen, Grand Island, NY, USA), Draq-5 (1:2000 dilution; Biostatus Limited, Shepshed, Leicestershire, UK), and fluorescein-labeled anti-αSMA (1:200 dilution; Sigma-Aldrich Corp., St. Louis, MO, USA) for 1 hour at room temperature in the dark. Sections were washed in 1X PBS or 1X TBS, then mounted with mounting media (10 mL PBS with 100 mg p-phenylenediamine to 90 mL glycerol; final pH 8.0).

Slides were imaged with a Zeiss LSM 780 confocal microscope (Carl Zeiss, Inc., Gottingen, Germany). For each experiment/comparison, all sections were stained simultaneously and imaged using identical configurations to ensure the validity of staining intensity comparisons. Under some circumstances, images were processed to optimize the brightness and/or contrast for optimal viewing on diverse computer screens. However, in all cases, any such adjustments were applied identically to both control and experimental images. At least six biological replicates were analyzed for each genotype.

Immunohistochemistry

Immunohistochemistry was used to detect pErk1/2 and pAkt levels in the lens as previously described,[29] using the CSA II Biotin-Free Tyramide Signal Amplification System (K150011-2; Dako Laboratories, Carpenteria, CA, USA) and CSA II Rabbit Link (K150180-2; Dako Laboratories), following the manufacturer's instructions (see Table 2 for the primary antibodies used). At minimum, three biological replicates were analyzed for each genotype.
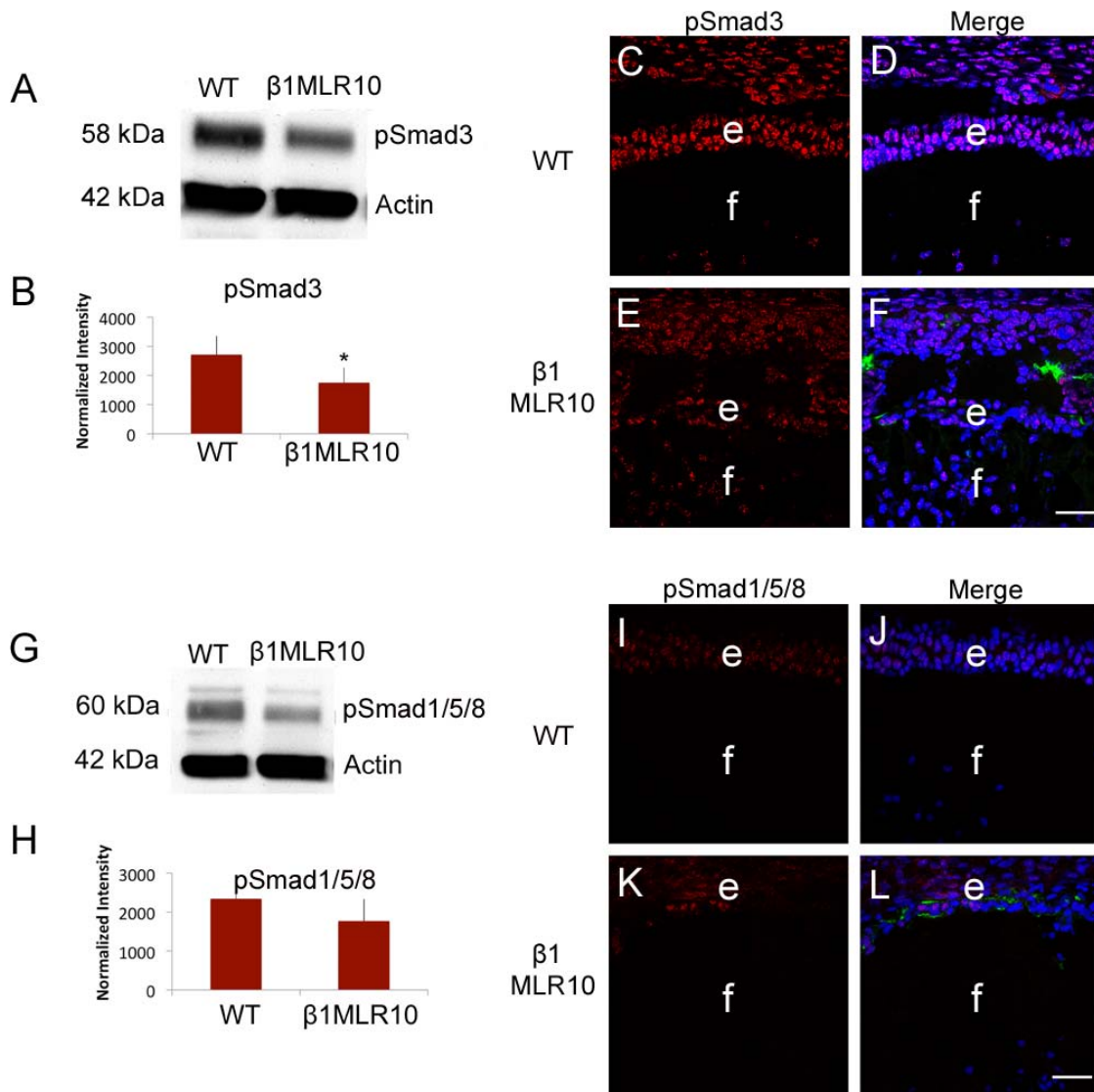
FIGURE 3. Analysis of Smad phosphorylation in E16.5 WT and β1MLR10 lenses. (A) Representative WB comparing pSmad3 levels in WT and β1MLR10 lenses. (B) Quantitation of the pSmad3 levels in WT and β1MLR10 lenses showing that pSmad3 levels were significantly lower in β1MLR10 lenses compared with WT (*$P = 0.023$, $n = 4$). (C–F) IF staining for pSmad3 (*red*) and αSMA (*green*) in WT (C, D) and β1MLR10 (E, F) lenses at E16.5. Qualitatively, pSmad3 staining was reduced in β1MLR10 LECs compared with WT. (G) Representative WB comparing pSmad1/5/8 levels between E16.5 WT and β1MLR10 lenses. (H) WB quantitation showing that pSmad1/5/8 levels in E16.5 WT and β1MLR10 lenses were not significantly different ($P = 0.18$, $n = 4$). (I–L) IF staining for pSmad1/5/8 (*red*) and αSMA (*green*) in WT (I, J) and β1MLR10 (K, L) lenses at E16.5. Qualitatively fewer LECs of β1MLR10 lenses had detectable levels of pSmad1/5/8 compared with WT. *Blue*, DNA; (C–F) *red*, pSmad3; (I–L) *red*, pSmad1/5/8; *green*, αSMA; e, epithelial cell; f, fiber cell. *Scale bar*: 38 μm.

RESULTS

RNA-Seq Identifies 120 Differentially Expressed Genes in E15.5 β1MLR10 Lenses

Deletion of β1-integrin from the lens after the completion of primary fiber cell elongation (E12.5-E13.5; β1MLR10) causes the lens epithelium to become grossly abnormal by E16.5.[26] Thus, RNA-seq was performed a day earlier, at E15.5, on β1MLR10 and WT lenses to identify changes in gene expression that might proximally drive the observed morphological alterations, while minimizing the detection of gene expression changes secondary to the phenotype. Analysis of the gene list confirms that the lens isolations included minimal contamination with nonlens ocular tissues, as *keratin 8* mRNA levels are very low in these samples (β1MLR10 lenses, 0.08

RPKM; WT lenses, 0 RPKM), which is expressed robustly in the cornea at this age.[19] Although we attempted to completely remove the adherent blood vessels (the tunica vasculosa lentis [TVL]) from these lenses, the RNA-seq suggests that the isolated lenses did likely retain some TVL, as low levels of *Pecam* mRNA (a blood vessel marker)[28] was detected in both WT (1.5 RPKM) and β1MLR10 (2.2 RPKM) lenses. However, this was unlikely to affect the analysis, as these levels were not significantly different between WT and mutant samples.

The RNA-seq analysis revealed that 5120 genes exhibit statistically significant ($P \leq 0.05$) differences in expression between E15.5 WT and β1MLR10 lenses. These genes were then subjected to previously developed stringent filtering criteria to prioritize candidates whose differential expression is likely to be biologically significant to the ocular lens.[28] These criteria are as follows: (1) potential DRGs are expressed at high
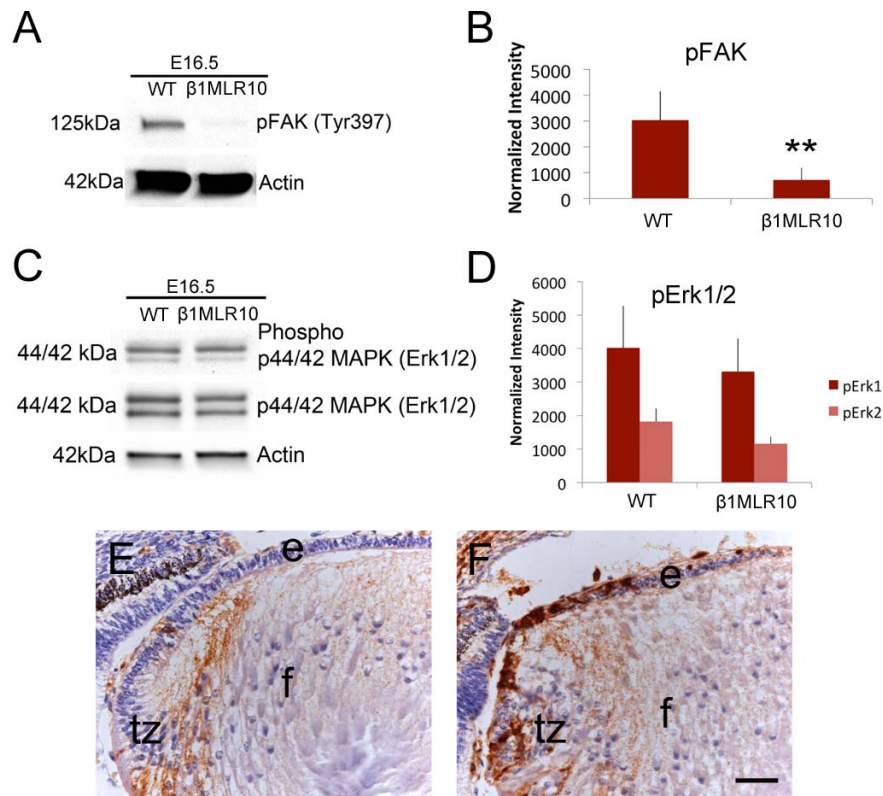
FIGURE 4. Analysis of pFAK and pErk1/2 levels in E16.5 WT and β1MLR10 lenses. **(A)** A representative WB comparing pFAK (Y397) levels between WT and β1MLR10 lenses. **(B)** WB quantitation showing that pFAK levels were significantly reduced in E16.5 β1MLR10 lenses compared with WT ($P \leq 0.001$, $n = 3$). **(C)** A representative WB comparing Erk1/2 and pErk1/2 levels between WT and β1MLR10 lenses. **(D)** WB quantitation showing that neither pErk1 nor pErk2 levels were significantly different in E16.5 β1MLR10 lenses compared with WT (pErk1 $P = 0.41$; pErk2, $P = 0.11$; $n = 4$). **(E, F)** IHC localization of pErk1/2 (*brown*) in E16.5 WT **(E)** and β1MLR10 **(F)** lenses. Both WT and β1MLR10 lenses exhibit pErk1/2 staining in in the newly formed lens fibers at the transition zone. However, β1MLR10 lenses also exhibit strong pErk1/2 staining in the lens epithelium (*arrows*), whereas little to no pErk1/2 is seen in the epithelial cells of WT lenses. *Blue*, DNA; *brown*, pErk1/2 **(E, F)**; e, lens epithelium; f, lens fiber cells; tz, transition zone. *Scale bar*: 39 μm.

enough levels in either the WT or β1MLR10 lens to plausibly affect cell function (unnormalized RPKM over 2); (2) the difference between WT and β1MLR10 lenses is greater than 2.5-fold to remove genes whose expression is different due to genetic background variations; and (3) exclusion of pseudogenes or unknown/predicted genes. This filtering resulted in a list of 120 DRGs (76 upregulated and 44 downregulated) that are plausibly involved in the phenotypic changes found in β1MLR10 lenses (Supplementary Table S1). Both the raw and processed RNA-seq data have been deposited in the Gene Expression Omnibus under accession number GSE77188.

Upregulated DRGs in β1MLR10 Lenses Include Genes Related to Cellular Stress and EMT Responses

The 120 prioritized candidate genes from the RNA-seq experiment were further analyzed by the bioinformatics tools PANTHER (http://www.pantherdb.org/),[30] IPA (Qiagen, Valencia, CA, USA, https://www.qiagenbioinformatics.com/products/ingenuity-pathway-analysis/) and DAVID (The Database for Annotation, Visualization and Integrated Discovery, http://david.abcc.ncifcrf.gov). For instance, according to PANTHER, these 120 genes can participate in 33 different pathways, which expectedly included apoptosis and integrin signaling pathways (Fig. 1; Supplementary Table S2). However, none of these tools identified common pathways shared by more than a

handful of the 120 genes, and many of the identified "pathways" were represented by only one gene, so these analyses did not give great insight into β1-integrin function in the lens (Fig. 1; Supplementary Table S2; data not shown).

The relative expression of each DRG in the lens compared with a mouse whole embryonic body (WB) reference dataset was determined using *iSyTE*,[31] which has previously been shown to effectively identify lens-enriched genes.[35] This analysis revealed that only 12 of the 76 upregulated and 7 of 44 downregulated DRGs exhibited enriched expression in the lens compared with reference (Supplementary Table S1). These findings suggest that β1-integrin is not a major regulator of lens-enriched gene expression after the completion of initial lens morphogenesis. Therefore, PubMed was used to interrogate the scientific literature, and relationships between the genes were manually assessed. This analysis revealed that 37 of the 76 upregulated DRGs are connected to either cellular stress responses, fibrosis or EMT in the scientific literature, whereas only 6 of the 44 downregulated genes had those connections (Table 3). The Fisher's exact test of independence suggest that the proportion of stress response, fibrotic, and EMT-related genes is significantly different ($P = 0.0001$) between upregulated and downregulated DRGs.

The time course of induction of four of these fibrotic/*EMT* marker genes (Table 3), chosen due to their RNA abundance (tissue plasminogen activator [*Plat*], *Mmp14*, and *Annexin A2* [*Anxa2*]) and/or importance as a marker of LEC EMT (*αSMA*), were investigated by qPCR of independent lens RNA samples
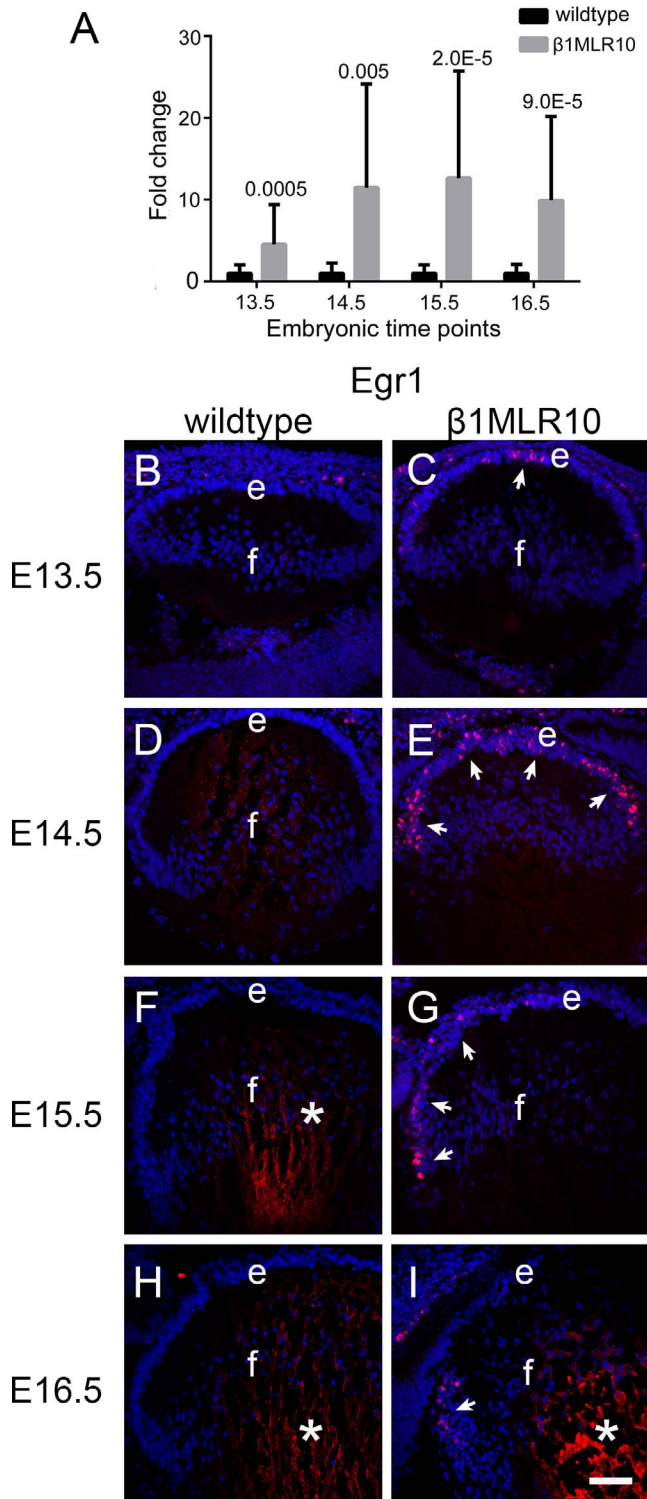
FIGURE 5. Developmental expression pattern of Egr1 in WT and β1MLR10 lenses. (**A**) qRT-PCR analysis of Egr1 mRNA in WT and β1MLR10 lenses from E13.5-E16.5, showing that Egr1 mRNA levels were significantly elevated in β1MLR10 lenses at all stages examined. (**B–I**) IF localization of Egr1 protein (*red*) in WT and β1MLR10 lenses from E13.5 to E16.5. At E13.5, no Egr1 protein was detected in WT (**B**) lenses, whereas a few Egr1-positive cell nuclei (*arrow*) were seen at the central epithelium of β1MLR10 lenses ([**C**] *arrows*). At E14.5, no Egr1 protein was detected in WT lenses (**D**); however, many Egr1-positive nuclei (*arrows*) were seen throughout the β1MLR10 lens epithelium. At E15.5, no Egr1 protein was detected in WT lenses (**F**); however, Egr1 protein was seen in numerous nuclei of the peripheral

(Fig. 2), starting at E13.5, proximal to the first total loss of β1-integrin protein from the β1MLR10 lens, and ending at E16.5, when the morphological defects are first consistently observed.[26] As predicted by RNA-seq, the mRNA levels for *αSMA*, the most commonly reported fibrotic marker in lens,[36,37] were significantly elevated by E14.5, and remained elevated at E16.5 (Fig. 2A), consistent with findings by IF[26] (Figs. 11B, 11E). *Anxa2*, a phospholipid-binding protein induced in numerous fibrotic conditions,[38–40] was significantly elevated by E13.5, and remained elevated later (Fig. 2B). *MT1-MMP* (encoded by *MMP14*) is a membrane-associated matrix metalloprotease that can activate latent TGF-β.[41] The precise levels of MT1-MMP are critical for normal tissue function, as it is induced in fibrosis,[42,43] but its absence also results in fibrosis due to defective collagen turnover.[44] Like *Anxa2*, *MMP14* mRNA levels are first elevated at E13.5 in β1MLR10 lenses, and they remain elevated later (Fig. 2C). *Plat* is a protease that can be a pro-fibrotic factor.[45] Its mRNA levels are also first elevated at E13.5 in β1MLR10 lenses, and these levels remain elevated later (Fig. 2D). Unfortunately, attempts to immunolocalize MMP14, Anxa2, and Plat were unsuccessful due to antibody limitations. Thus, it is unknown whether these mRNA differences are reflected at the protein level.

Phosphorylated Smad Signaling Is Not Elevated in E16.5 β1MLR10 Lenses

In the lens, EMT is best understood to be mediated by elevated Smad2/3 phosphorylation, driven by TGF-β signaling.[36] However, WB detected a reduction in Smad3 phosphorylation (Figs. 3A, 3B) in β1MLR10 lenses at E16.5, which was also validated by IF analysis comparing phosphorylated Smad3 (pSmad3) levels between WT (Figs. 3C, 3D) and β1MLR10 lenses (Figs. 3E, 3F). Because we recently found that deletion of β1-integrin from the lens vesicle resulted in ectopic activation of Smad1/5/8 phosphorylation in the lens epithelium by E12.5,[15] we also evaluated pSmad1/5/8 levels in β1MLR10 lenses. By WB (Figs. 3G, 3H), pSmad1/5/8 levels were not significantly changed in E16.5 β1MLR10 lenses, and by IF, fewer pSmad1/5/8 positive nuclei were detected in β1MLR10 lenses (Figs. 3K, 3L) than WT (Figs. 3I, 3J). The downregulation of pSmad3 and pSmad1/5/8 labeling in E16.5 β1MLR10 lenses appears to contradict our prior observation[26] that nuclear Smad4 levels are elevated in this tissue but may reflect the difference between evaluating levels of an active (pSmad3 or pSmad1/5/8) protein form versus total levels of a protein that interacts with many different Smads (Smad4). Evaluation of both pSmad3 and pSmad1/5/8 distribution in the lens before E16.5 revealed no obvious differences between WT and β1MLR10 lenses (data not shown). Overall, these findings suggest that the mechanism underlying the pathology of β1MLR10 lenses is independent of either TGFβ-driven elevations in Smad2/3 phosphorylation or BMP-driven activation of Smad1/5/8. We then proceeded to investigate other signal transduction cascades that may be responsible for the pathology of the β1MLR10 lens.

β1MLR10 lens epithelium ([**G**] *arrows*). At E16.5, no Egr1 protein was detected in WT lenses (**H**), whereas Egr1 protein was detected in islands of nuclei in the LECs closest to the transition zone of β1MLR10 lenses (*arrow*). (**B–I**) *Blue*, DNA; *red*, Egr1; e, epithelial cell; f, fiber cell. *Scale bar*: 71 μm. *Error bars* in (**A**) represent SD. Statistical significance was determined with nested ANOVA and is given above the *error bar* in the figure. *Nonspecific staining as determined by nonnuclear distribution and its presence in WT lenses that express very little Egr1 mRNA.

A

Mmusculus-JASPAR_CORE-Egr1-MA0162.1
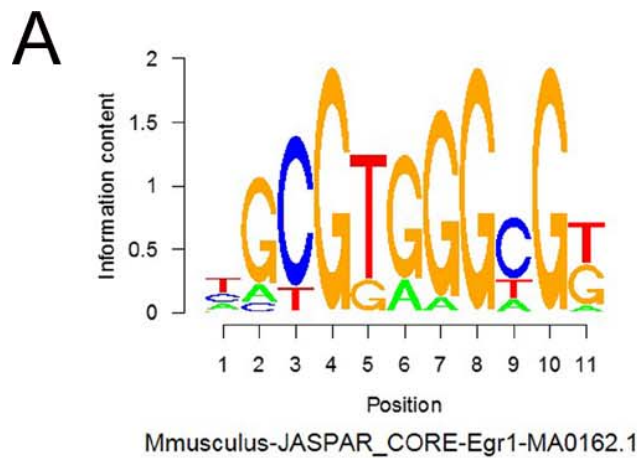
B

Gene	Entrez ID	Motif sequence (5' to 3')	Start	End
Akr1b8	14187	GGCGGGGGCGG	-65	-55
Alox12	11684	TGTGAGGGCGG	-55	-45
Bcam	57278	GGGGTGGGCGT	-44	-34
Ccbe1	320924	TGCGTGAGTGA	-800	-790
Ccdc109b	66815	GGCGGGGGTGG	-1116	-1106
Ccdc85c	668158	GGGGTGGGCGG	-27	-17
Cited4	56222	AGAGTGGGCGT	-50	-40
D8Ertd82e	244418	TGCGGGGGTGC	-61	-51
Dctd	320685	GGCGGGGGCGC	-1432	-1422
Hjurp	381280	TGCGTGGGCAT	-738	-728
Hmga1	15361	CGCGGCGGCGG	-72	-62
Hmgn2	15331	GGCGGGGGTGG	-955	-945
Hspa8	15481	AGCGGGGGCGA	-224	-214
Htr1d	15552	GGTGGGGGCGG	-71	-61
Lars2	102436	GGCCTGGGCGG	-133	-123
Paqr7	71904	AATGTGGGCGT	-751	-741
Rab6b	270192	GGCGCGGGCGG	-315	-305
Rpl29	19944	TGAGTGGGTGG	-1577	-1567
Tagap1	380608	CGCGTGAGGGG	-75	-65
Thbs1	21825	TGCGTGGGCGG	-242	-232
Upp1	22271	CTCGTGGGAGG	-279	-269
Acta2	11475	CGAGTGGGAGG	-19	-9
Bend6	320705	TGCGCGCGCGG	-130	-120
Col26a1	140709	GGCGTGGGCGC	-76	-66
Crabp2	12904	GGCGGGGGCGG	-60	-50
Crip1	12925	GGCGGGGGCGG	-30	-20
Cyr61	16007	TGTGTGGGAGG	-1309	-1299
Dynlt1b	21648	AGCGTAGGTGG	-14	-4
Egr1	13653	GGCGGAGGCGG	-59	-49
Fcer1g	14127	AGTGTGGGCGA	-24	-14
Fgf15	14170	GGCCTGGGCGG	-157	-147
Glipr2	384009	TGGGCGGGCGT	-1129	-1119
Hebp1	15199	CACGTGGGTGG	-57	-47
Hemk1	69536	CACGTGGGTGA	-363	-353
Klf4	16600	TGCGAGTGCGT	-868	-858
Mmp14	17387	GGCGGGGGCGG	-23	-13
Mmp2	17390	TGTGTGGGGGG	-608	-598
Mt1	17748	TGTGTGGGGGG	-968	-958
Nab1	17936	GGCGGGGGAGG	-20	-10
Nab2	17937	GGCGTGGGCGG	-271	-261
Nes	18008	TGCATGGGCGT	-2045	-2035
Nmb	68039	TGTGTGGGCGG	-68	-58
Npw	381073	GGCGGGGGCGA	-151	-141
Pak1	18479	GGCTTGGGCGG	-42	-32
Phlda3	27280	AGTGTGGGTGG	-1804	-1794
Phpt1	75454	AGTGTGGGCGG	-1349	-1339
Plagl1	22634	TGCGTGGGAGC	-87	-77
Plekha2	83436	GGCGTTGGCGA	-318	-308
Rcan2	53901	AGGGTGGGAGG	-1209	-1199
Rprm	67874	AGGGTGGGTGG	-936	-926
Tnfrsf12a	27279	GGCGGGGGCGG	-48	-38
Zdhhc2	70546	GGCGGGGGCGG	-46	-36

β1MLR10 Lenses Exhibit a Reduction in Phosphorylated Focal Adhesion Kinase (pFAK), While pErk1/2 and pAkt Levels Are Elevated in LECs

Integrin activation is known to induce the phosphorylation of FAK, which is abundantly expressed in the developing lens,[46] and plays a role in lens fiber cell morphogenesis.[47] WB revealed a near complete absence of pFAK[tyr397] in E16.5 β1MLR10 lenses (Figs. 4A, 4B). Because FAK is known to be upstream of MAP kinase (MAPK) signaling,[48,49] the levels of Erk1/2 and pErk1/2 (Figs. 4C, 4D) were then assessed in WT and β1MLR10 lenses. However, by WB of whole lenses, neither Erk1/2 (Fig. 4C, quantitation not shown) nor pErk1/2 (Figs. 4C, 4D) levels were significantly altered in whole lenses of E16.5 β1MLR10 mice. We hypothesized that because lens fibers, which contribute to most of the cellular mass of the lens, have high levels of pErk1/2 due to the FGF signaling required for their differentiation,[43,50,51] the evaluation of whole lenses may mask expression changes specifically exhibited by β1MLR10 LECs. Therefore, we also evaluated pErk1/2 levels in E16.5 LECs via immunohistochemistry (IHC). Notably, this analysis revealed that pErk1/2 levels are strikingly elevated in E16.5 β1MLR10 LECs (Fig. 4F, arrows) compared with WT (Fig. 4E).

Because pErk1/2 levels were elevated in β1MLR10 lenses, we also tested Akt phosphorylation (pAkt) levels in E16.5 mutant and WT lenses using IHC. Similar to pErk1/2, pAkt is elevated in the LECs of β1MLR10 lenses compared with WT (data not shown).

β1MLR10 Lenses Exhibit Upregulation of the Immediate Early Response TF, Egr1

The Ras/MAPK/Erk pathway is able to directly reprogram cellular behavior via upregulation of immediate early response (IER) TFs.[52,53] Notably, three of the genes upregulated in β1MLR10 lenses, *Fos*, *Junb*, and *Egr1* (Table 3), are IER TFs whose mRNA levels are directly regulated via diverse signal transduction cascades, including the MAPK pathway.[53,54] Of these, Egr1 was selected for further study because not only was it expressed at the highest levels of the three IER genes, it was also among the most upregulated (10-fold) genes overall in β1MLR10 lenses (Table 3).

Next, the time course of Egr1 upregulation relative to the loss of β1-integrin protein from the β1MLR10 lens was evaluated by qRT-PCR and immunolocalization (Fig. 5). *Egr1* mRNA levels are significantly elevated shortly after the loss of β1-integrin protein from the lens at E13.5,[26] and Egr1 mRNA levels remain elevated until at least E16.5 (Fig. 5A). *Egr1* protein was generally not detected in WT lenses between E13.5 and 16.5 (Figs. 5B, 5D, 5F, 5H). Consistent with the transcript-level analysis, Egr1-positive nuclei (arrows) were observed in the central epithelium of β1MLR10 lenses at E13.5 (Fig. 5C), and most of the lens epithelium at E14.5 (Fig. 5E). At E15.5 and E16.5, most Egr1-positive cell nuclei were confined

FIGURE 6. The putative promoters of genes differentially regulated in β1MLR10 lenses are enriched in Egr1 DNA-binding motifs. (A) Sequence logo for the JASPAR core Egr1 binding site based on the previously reported Egr1 position weight matrix.[188] (B) Motif enrichment analysis revealed a statistically significant enrichment of Egr1 DNA-binding motifs in the putative regulatory regions 2.5 kb upstream of TSS of DRGs identified in β1MLR10 lenses. The start and end positions of the promoter region that matches the Egr1 DNA-binding motif (5' to 3'; position relative to TSS) for each candidate DRG are given. Upregulated DRGs are indicated in *red*, and downregulated DRGs are indicated in *green*.

Investigative Ophthalmology & Visual Science

TABLE 2. List of Antibodies Used for IF Staining, IHC Staining, and WB

	Primary Antibodies	Fixation	Blocking Buffer	Dilution Buffer	Incubation Condition and Dilution Rate
Antibodies for IF	β1-integrin (MAB 1997, Millipore)	1:1 acetone-methanol	2% BSA in PBS	2% BSA in PBS	1 h at room temperature, 1:200
	α-SMA (1A4 F3777, Sigma-Aldrich Corp.)	1:1 acetone-methanol	2% BSA in PBS	2% BSA in PBS	1 h at room temperature, 1:200
	Aquaporin0 (AB3071, Millipore)	1:1 acetone-methanol	2% BSA in PBS	2% BSA in PBS	Overnight at 4°C, 1:200
	Cleaved Caspase 3 (9661, Cell Signaling)	4% PFA	2% BSA and 5% goat serum in TBS	2% BSA and 5% goat serum in TBS	Overnight at 4°C, 1:100
	cMaf (sc-7866, Santa Cruz)	1:1 acetone-methanol	2% BSA in PBS	2% BSA in PBS	1 h at room temperature, 1:100
	Prox1, Polyclonal antibody produced in house against homeo-Prospero domain; validated on Prox1 null lenses[29]	1:1 acetone-methanol	2% BSA in PBS	2% BSA in PBS	1 h at room temperature, 1:500
	Egr1 (4153, Cell Signaling; antibody validated on injured Egr1-null lenses (unpublished data)	4% PFA	5% goat serum, and 0.3% Triton X-100 in PBS	2% BSA, and 0.3% Triton X-100 in PBS	Overnight at 4°C, 1:400
	pSmad3 (clone EP823Y, Epitomics)	4% PFA	2% BSA, 10% goat serum and 0.1% Triton X-100 in TBS	2% BSA, 10% goat serum, and 0.1% Triton X-100 in TBS	Overnight at 4°C, 1:100
	pSmad1/5/8 (sc-12353, Santa Cruz Biotechnology)	4% PFA	5% goat serum and 2% BSA in PBS	5% goat serum and 2% BSA in PBS	1 h at room temperature, 1:50
	Nab2 (19601-1-AP, Proteintech)	4% PFA	5% goat serum, 0.3% Triton X-100 in PBS	2% BSA, 0.3% Triton X-100 in PBS	Overnight at 4°C, 1:100
Antibody for IHC	pAkt (9271s, Cell Signaling)	Paraffin section	2% BSA in TBST	2% BSA in TBST	Overnight at 4°C, 1:50
	pErk (4377s, Cell Signaling)	Paraffin section	2% BSA in TBST	2% BSA in TBST	Overnight at 4°C, 1:50
Antibodies for WB	p44/p42 MAPK (Erk1/2) (9102, Cell Signaling)	-	-	-	1:1000
	Phospho-p44/p42 MAPK (pErk1/2) (Thr202/Tyr204) (9101, Cell Signaling)	-	-	-	1:1000
	pFAK (Y397) (3283, Cell Signaling)	-	-	-	1:1000
	p-Smad3 (Ser423/Ser425) (P8402, Millipore)	-	-	-	1:1000

Dashes indicate that these steps are for IF and IHC only, which were not included during WB. PFA, paraformaldehyde.
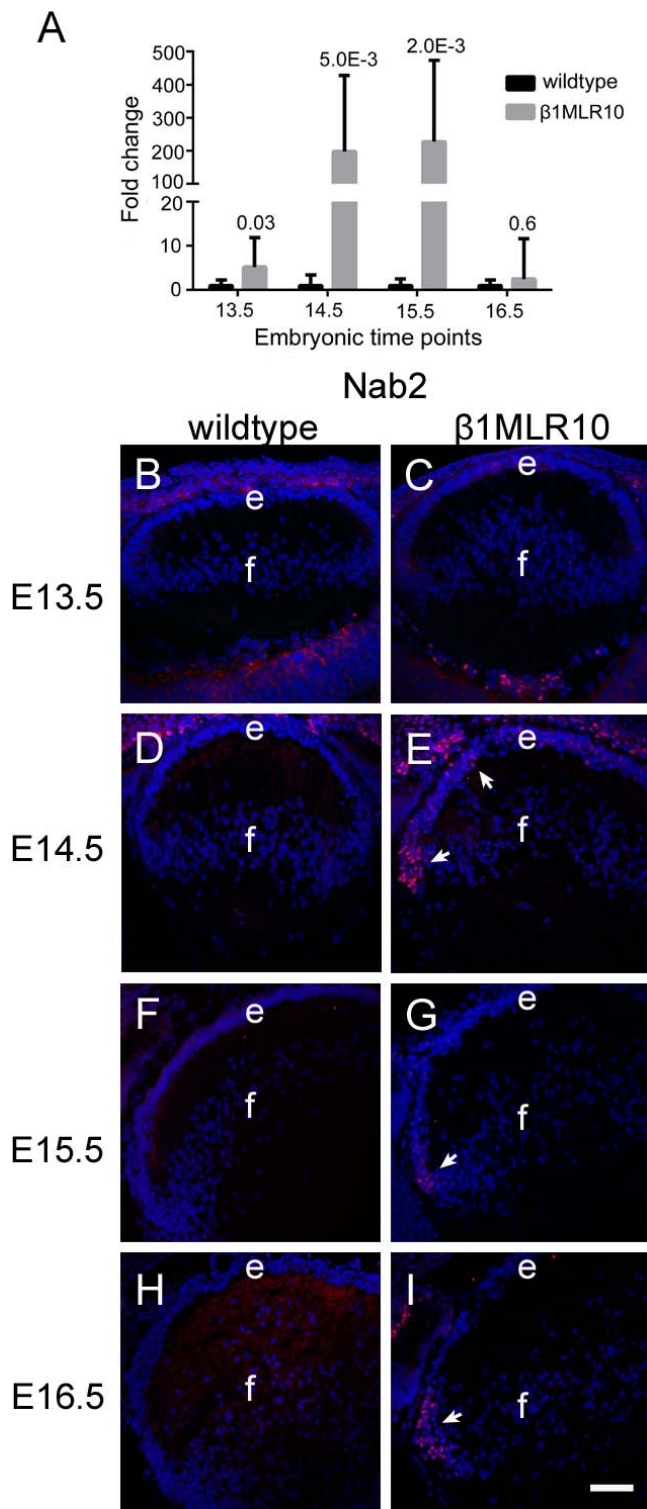
FIGURE 7. Developmental expression pattern of Nab2 in WT and β1MLR10 lenses. (**A**) qRT-PCR analysis of Nab2 mRNA in WT and β1MLR10 lenses from E13.5 to E16.5, showing that Nab2 mRNA levels were significantly elevated in β1MLR10 lenses between E13.5 and E15.5, whereas these levels were similar in WT at E16.5. (**B–I**) IF localization of Nab2 protein (*red*) in WT and β1MLR10 lenses from E13.5 to E16.5. At E13.5, no Nab2 protein was detected in either WT (**B**) or β1MLR10 lenses (**C**). At E14.5, no Nab2 protein was detected in WT lenses (**D**); however, Nab2-positive nuclei (*arrows*) were seen in the peripheral β1MLR10 lens epithelium. At E15.5, no Nab2 protein was detected in WT lenses (**F**); however, Nab2 protein was seen in a few nuclei of the peripheral β1MLR10 lens epithelium (**G**, *arrow*). At
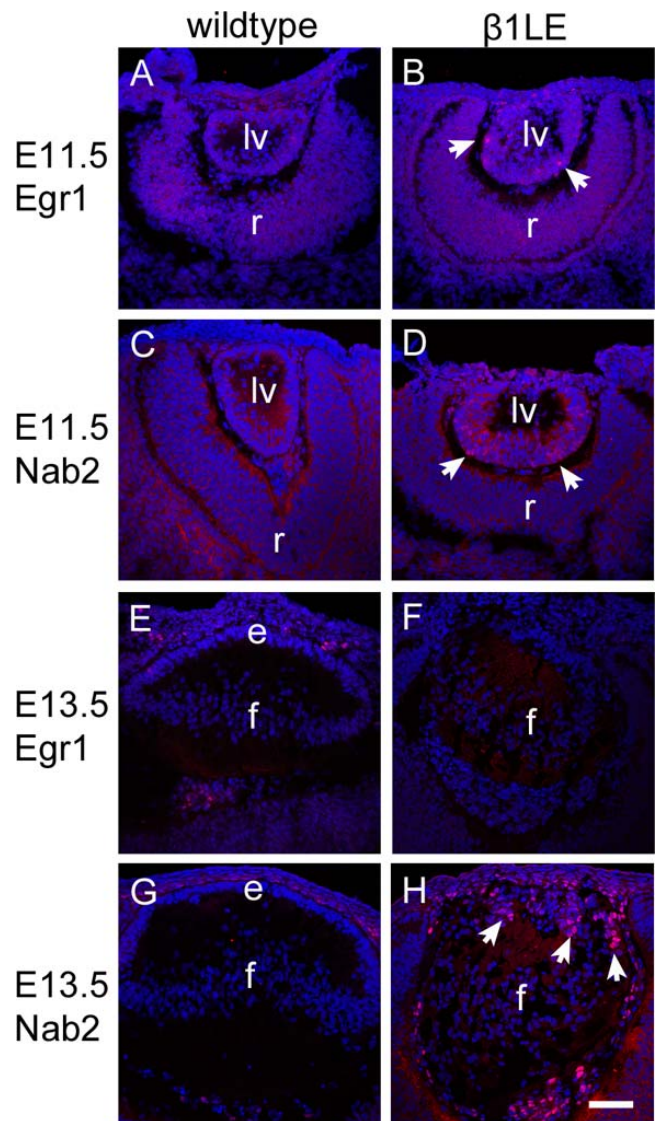
FIGURE 8. Developmental expression pattern of Egr1 and Nab2 in WT and β1LE lenses. (**A–D**) Sections from E11.5 eyes stained for Egr1 (*red*, [**A**, **B**]) and Nab2 (*red*, [**C**, **D**]). (**A**) WT lenses lack Egr1 immunoreactivity at E11.5, whereas (**B**) Egr1-positive nuclei (*arrows*) were detected in the lens vesicle of E11.5 β1LE lenses. (**C**) No Nab2 immunostaining was detected in WT lenses at E11.5. (**D**) Nab2-positive nuclei (*arrows*) were found in the lens vesicle of E11.5 β1LE lenses. (**E–H**) Sections from E13.5 eyes stained for Egr1 (*red*, [**E**, **F**]) and Nab2 (*red*, **G**, **H**). Both WT (**E**) and β1LE lenses (**F**) showed no Egr1 immunoreactivity at E13.5. (**G**) No Nab2 immunostaining was observed in WT lenses at E13.5, whereas (**H**) many Nab2-positive nuclei (*arrows*) were found in the abnormally differentiating fiber cells in E13.5 β1LE lenses. (**A–H**) *Blue*, DNA; (**A**, **B**) and (**E**, **F**) *red*, Egr1; (**C**, **D**) and (**G**, **H**) *red*, Nab2; lv, lens vesicle; r, retina; e, lens epithelium; f, lens fibers. *Scale bar*: 71 μm (**A–H**).

E16.5, no Nab2 protein was detected in WT lenses (**H**), whereas Nab2 protein was detected in islands of nuclei in the LECs closest to the transition zone of β1MLR10 lenses (*arrow*). (**B–I**) *Blue*, DNA; *red*, Nab2; e, epithelial cell; f, fiber cell. *Scale bar*: 71 μm. *Error bars* in (**A**) represent SD. Statistical significance was determined with nested ANOVA and is given above the *error bar* in the figure.
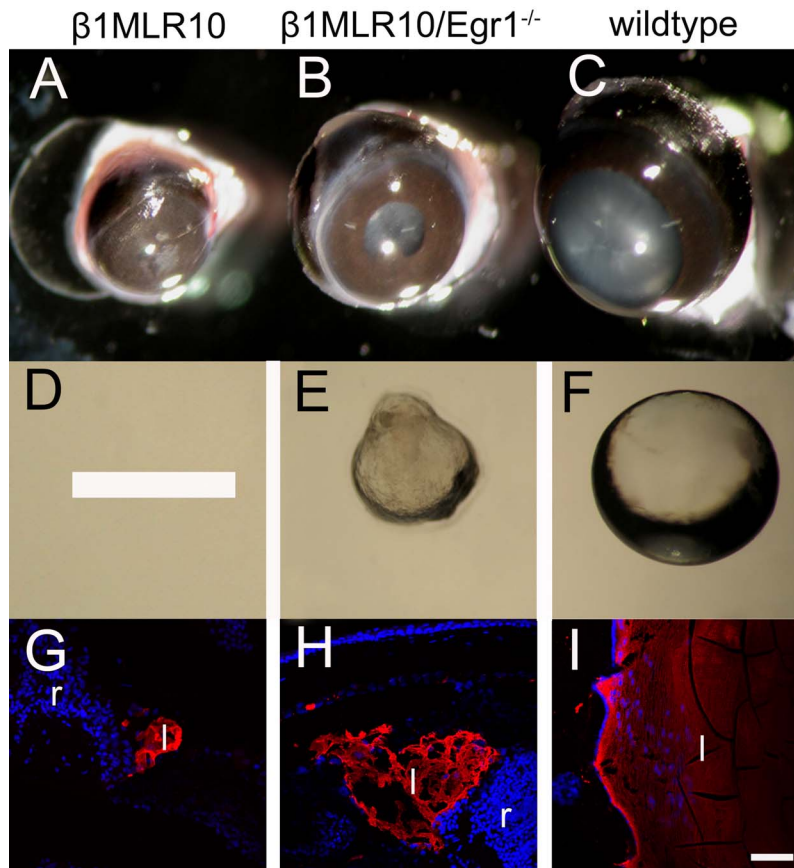
FIGURE 9. Deletion of Egr1 from β1MLR10 mice partially rescues the lens phenotype. (**A**) An eye isolated from a 2-month-old β1MLR10 mouse. (**B**) An eye isolated from a β1MLR10/Egr1$^{-/-}$ mouse, showing that the microphthalmia is less severe in mice lacking Egr1. (**C**) An eye isolated from a WT mouse showing the relative size of a normal mouse eye. (**D**) No lens tissue was isolatable from β1MLR10 eyes via dissection. (**E**) Bright-field micrograph of a lens isolated from a 2-month-old β1MLR10/Egr1$^{-/-}$ mouse, showing that it is smaller than normal and not transparent. (**F**) Bright-field micrograph of a lens isolated from a 2-month-old WT mouse. (**G**) IF detection of Aquaporin0 (*red*) in a section from a 2-month-old β1MLR10 eye, showing that these eyes contain very few cells expressing the marker of lens fiber cells at this age. (**H**) IF detection of Aquaporin0 (*red*) in a section from a 2-month-old β1MLR10/Egr1$^{-/-}$ eye, showing that these eyes have much more tissue staining for aquaporin0 (*red*), although the lens is still profoundly abnormal. (**I**) IF detection of aquaporin0 (*red*) in a section from a 2-month-old WT eye, showing the normal distribution of aquaporin0 in lens fibers. (**G–I**) *Blue*, DNA; *red*, Aquaporin0; l, lens; r, retina. *Scale bar*: 71 μm.

to the peripheral lens epithelium (Figs. 5G, 5I) in β1MLR10 lenses.

Egr1 Binding Sites Are Present and Enriched in Genes Upregulated in β1MLR10 Lenses

Next, to investigate the molecular connection between upregulation of IER transcription factors and the other genes misregulated in the β1MLR10 lens, we took two approaches: (1) examine if any TF-binding motifs were enriched in the DRGs; and (2) specifically analyze if the Egr1 motif is overrepresented in the putative promoters of the DRGs. The iRegulon package[32] was used to identify the enrichment of known TF-binding motifs in the putative regulatory region (10 kb total sequence analyzed from −5kb to +5kb of the TSS of the 120 β1MLR10 lens DRGs. This analysis identified enrichment and overrepresentation of binding sites for Cys2His2 TFs (such as Egr1), leucine zipper TFs (such as the AP1 factors Fos and Junb), and members of the Ets domain family (which encode direct transcriptional effectors of Erk phosphorylation)[55] (Table 4) in these putative regulatory regions. Further, iRegulon analysis identified overrepresentation of Egr1 binding sites in 38% (46/120) of the DRGs, including 32 of the

upregulated and 14 of the downregulated candidates with a significant (≥3) NES of 5.8 (Table 4).

Egr1 is a multifunctional TF that regulates cellular stress, apoptosis, and fibrosis in different contexts.[56-59] As Egr1 is upregulated in β1MLR10 lenses and its binding sites were also overrepresented in the putative regulatory regions of β1MLR10 lens DRGs, we performed a detailed analysis to determine the presence of Egr1 binding motifs in the putative promoters of these genes irrespective of their enrichment. Thus, a 2.5-kb region upstream of the TSS of all 120 DRGs was analyzed for putative Egr1 binding motifs using the JASPAR position weight matrix[33] for Egr1, CORE-Egr1-MA0162.1 (Fig. 6A). This analysis revealed that the 5′ flanking sequence of 31 of the 76 upregulated DRGs and 21 of the 44 downregulated DRGs contained consensus Egr1 binding motifs (Fig. 6B). To gain further insight into potential molecular connections between Egr1 and the DRGs, we examined the scientific literature to identify β1MLR10 lens DRGs that may have published connections with this transcriptional regulator. We find 18 of the 76 upregulated DRGs to be either regulated by or coregulated with Egr1 (see Table 3, Supplementary Table S1). In contrast, only 1 of the 44 downregulated DRGs has a previously described connection with Egr1. Among the 19 DRGs with prior evidence connecting them with Egr1, 8 are
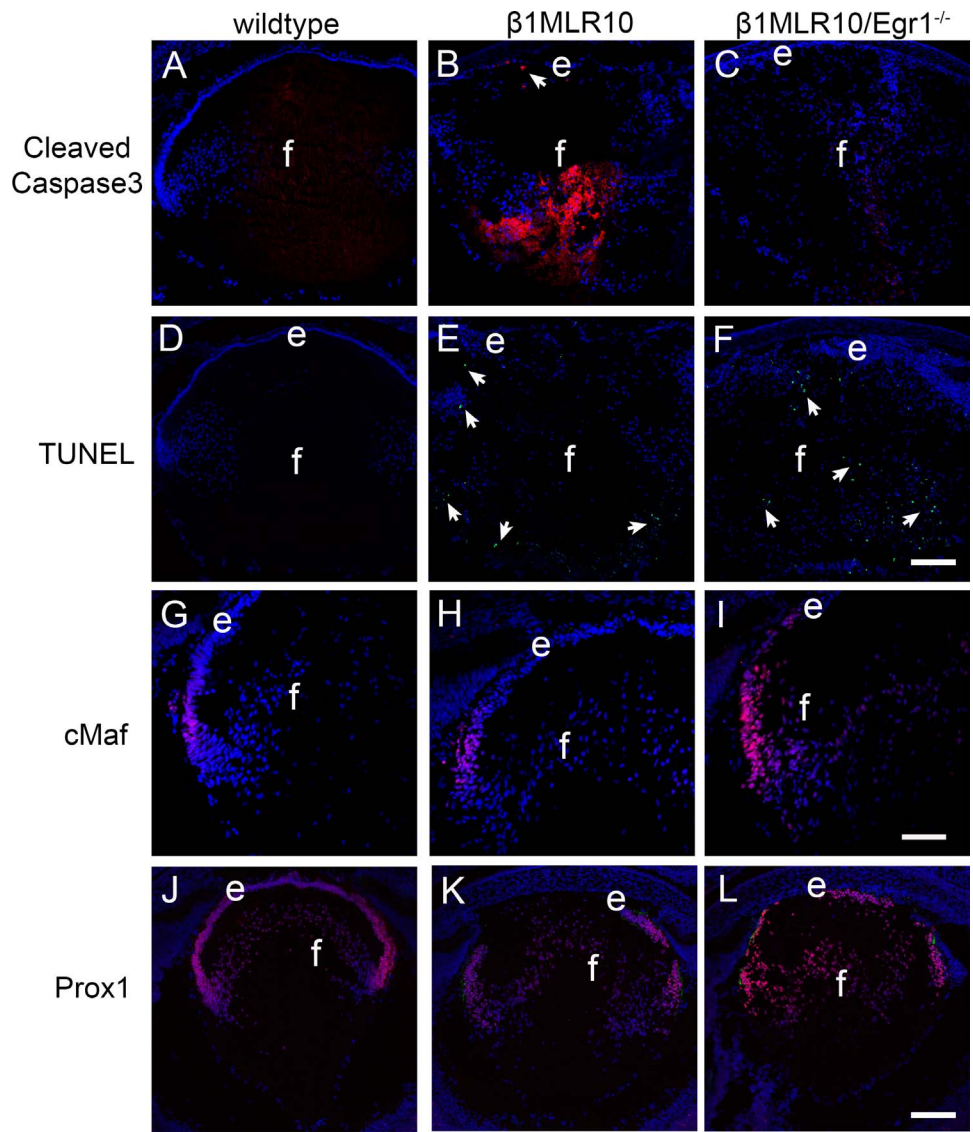
FIGURE 10. Analysis of apoptosis and fiber cell differentiation markers in β1MLR10/Egr1$^{-/-}$ lenses. (**A–C**) IF of cleaved Caspase 3 (*red*) in newborn lenses. WT lenses (**A**) exhibit no cleaved Caspase 3 immunoreactivity under the conditions used. Intense cleaved Caspase 3 immunoreactivity was seen in both the lens fibers and epithelium (*arrow*) of β1MLR10 lenses (**B**), whereas little to no cleaved Caspase 3 immunoreactivity was seen in newborn β1MLR10/Egr1$^{-/-}$ lenses (**C**). (**D–F**) TUNEL staining of newborn lenses. WT lenses exhibit no TUNEL-positive nuclei (*green*) at birth (**D**), whereas TUNEL staining was detected in both the epithelial cells and fibers of both β1MLR10 (**E**) and β1MLR10/Egr1$^{-/-}$ lenses (**F**) (*arrows*). (**G–I**) Immunolocalization of cMaf in E16.5 lenses. WT lenses (**G**) exhibit strong cMaf labeling in the transition zone nuclei in the midst of differentiating into lens fiber cells. cMaf staining is seen in a similar pattern in β1MLR10 lenses, although the number of positive nuclei appears expanded (**H**). β1MLR10/Egr1$^{-/-}$ lenses (**I**) appear to exhibit brighter cMaf staining overall, and this staining extends farther into the lens epithelium than either WT or β1MLR10 lenses. (**J–L**) Immunolocalization of Prox1 in E16.5 lenses. WT lenses (**J**) exhibit strongest Prox1 labeling in the transition zone nuclei in the midst of differentiating into lens fiber cells, whereas some Prox1 protein is detected in LECs at this age. Prox1 staining is seen in a similar pattern in β1MLR10 lenses, although positive nuclei are brighter in LECs than in control (**K**). β1MLR10/Egr1$^{-/-}$ lenses (**I**) stain more intensely for Prox1 immunoreactivity in LECs than either WT or β1MLR10 lenses. (**A–L**) *Blue*, DNA; (**A–C**) *red*, cleaved Caspase 3; (**D–F**) *green*, TUNEL positive; (**G–I**) *red*, cMaf; (**J–L**) *red*, Prox1; e, epithelial cells; f, fiber cells. (**A–F**) *Scale bar*: 142 μm; (**G–I**) *scale bar*: 62 μm; (**J–L**) *scale bar*: 142 μm.

validated as direct Egr1 target genes in other cells or tissues (Table 3).

The Established Egr1 Target Gene Nab2 Is Upregulated in β1MLR10 Lenses

Interestingly, Ngfi-A binding protein 2 (Nab2), which exhibits the highest extent of upregulation (14-fold) among these eight known Egr1 direct target genes (Fig. 6B; Table 3), is known to be intricately involved in Egr1 function. Nab2 participates in a negative feedback loop to downregulate Egr1 expression, thus limiting the IER,[58–60] while simultaneously stimulating Egr1-mediated transcription at promoters with weak Egr1 binding sites.[61,62] Therefore, we investigated the expression pattern of Nab2 in β1MLR10 lenses (Fig. 7). Nab2 transcript levels were significantly upregulated at E13.5, exhibit a further sharp elevation at E14.5, and remain elevated in E15.5 β1MLR10 lenses (Fig. 7A). By immunolocalization, no Nab2 protein was detected in the WT lens at any stage examined (Figs. 7B, 7D, 7F, 7H). Although Nab2 protein was not detected in the β1MLR10
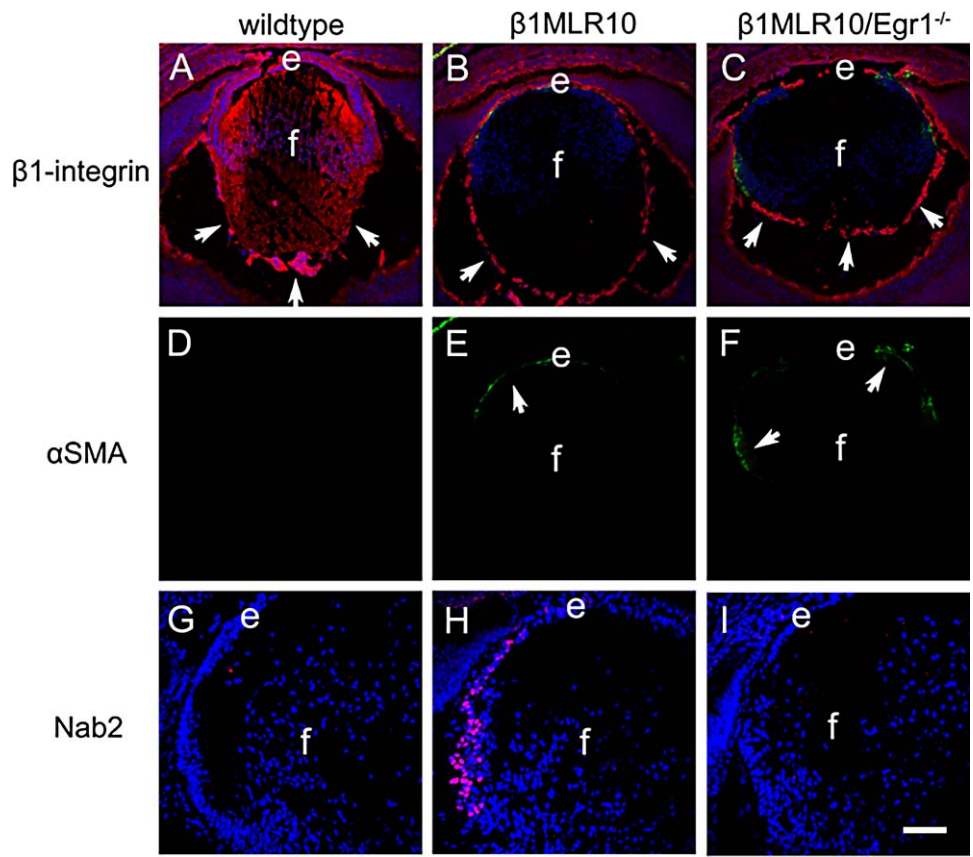
FIGURE 11. Molecular phenotype of β1MLR10/Egr1$^{-/-}$ lenses. (A–C) Sections from E16.5 eyes stained for β1-integrin (*red*) and α-smooth muscle actin (*green*). E16.5 WT lenses (A) exhibit β1-integrin immunoreactivity (*red*) in both lens epithelium and fiber cells. The intense β1-integrin staining at the lens periphery is in the tunica vasculosa (*arrows*). E16.5 β1MLR10 (B) and β1MLR10/Egr1$^{-/-}$ (C) lenses lack β1-integrin immunoreactivity in lens tissue, but retain the intense β1-integrin immunoreactivity in the tunica vasculosa (*arrows*). (D–F) The αSMA (*green*) channel alone of the images shown in (A–C). No αSMA immunoreactivity was detected in WT lenses (D) at E16.5; however, both β1MLR10 (E) and β1MLR10/Egr1$^{-/-}$ (F) lenses exhibit αSMA immunoreactivity (*green, arrows*). (G–I) Sections from E16.5 eyes stained for Nab2. (G) WT lenses lack Nab2 immunoreactivity at E16.5. (H) Nab2-positive nuclei are detected in the peripheral epithelium of E16.5 β1MLR10 lenses. (I) No Nab2 immunostaining was detected in β1MLR10/Egr1$^{-/-}$ lenses. (A–C and G–I) *Blue*, DNA; (A–F) *green*, αSMA; (A–C) *red*, β1-integrin; (G–I) *red*, Nab2; e, lens epithelium; f, lens fibers. *Scale bar*: 142 μm (A–F); *scale bar*: 71 μm (G–I).

lens at E13.5 (Fig. 7C), islands of cells exhibiting nuclear localized Nab2 (arrows) were present in peripheral LECs at E14.5 to E16.5 (Figs. 7E, 7G, 7I). This confirmed that the known Egr1 target Nab2 is also upregulated in β1MLR10 lens, giving insight into the molecular consequence of Egr1 upregulation that results from β1 integrin deletion in the β1MLR10 lens.

Egr1 and Nab2 Are Also Upregulated Early After β1 Integrin Deletion in β1LE Lenses

Previously, we found that deletion of β1 integrin from the lens vesicle (β1LE mice) results in a complete transition of the lens epithelium to fiber cells.[15] Because upregulation of the Egr1/Nab2 genes is a significant molecular consequence of β1-integrin deletion from β1MLR10 lenses, we sought to test the universality of this finding between the early and late β1 integrin deletion mutants by examining Egr1 expression in β1LE lenses at E11.5, proximal to the loss of β1-integrin protein from the lens, as well as at E13.5, when the β1LE phenotype is seen. While occasional Egr1-positive cell nuclei were detected in WT E11.5 (Fig. 8A) lenses, numerous Egr1-positive nuclei (arrows) were observed in β1LE lens vesicles (Fig. 8B); however, by E13.5, neither WT (Fig. 8E) nor β1LE (Fig. 8F) lenses exhibited Egr1 staining. We also tested the levels of

Nab2 in β1LE lenses. Although no nuclear Nab2 staining was detected in WT lenses at either E11.5 (Fig. 8C) or E13.5 (Fig. 8G), β1LE lenses exhibited nuclear Nab2 staining in subsets of cell nuclei throughout the lens vesicle at E11.5 (Fig. 8D) and in the remaining anterior lens cells at E13.5 (Fig. 8H), which have not completely yet transformed to lens fibers. Thus, β1 integrin deletion from the lens vesicle also led to the upregulation of Egr1 and its target Nab2 in the lens, although this was restricted to times proximal to β1 integrin deletion.

Egr1 Deletion Partially Rescues the β1MLR10 Phenotype

Because the bioinformatics and experimental analyses suggested that Egr1 is likely involved in the regulation of several β1MLR10 lens DRGs (Table 3), we sought to determine whether deletion of *Egr1* was sufficient to ameliorate the consequences of β1-integrin loss from the lens. Therefore, we generated mice that lacked both the *β1-integrin* and *Egr1* genes from the lens (β1MLR10/Egr1$^{-/-}$). As previously reported, adult β1MLR10 mice lack externally visible eyes, which are severely microphthalmic (Fig. 9A) with little to no identifiable lens tissue on dissection (Fig. 9D), although small islands of cells stain positive for the lens fiber marker, Aquaporin0 (Fig. 9G; $n = 6$). In contrast, the eyes of adult

Investigative Ophthalmology & Visual Science

Table 3. Genes Differentially Expressed in E15.5 β1MLR10 Lenses as Determined by RNA-seq That Have Published Relationships With Fibrosis and/or Stress Responses

Gene ID	Gene Description	Fold Change From WT	FDR, P Value	β1-MLR10 Mean RPKM	WT Mean RPKM	Lens Enrichment iSyTe at E12.5 1.5 Cutoff	Predicted Egr1 Motif in Promoter	Functional Connection With Egr1	Biological Function
Eif3j2	Eukaryotic translation initiation factor 3, subunit J2	369	4.90E-114	5.96	0.01	np	No	nr	Regulates translational control during nutrient depletion[101]; selects AUG start codons[102]
Mt1	Metallothionein 1	296	0.00E+00	447.52	1.49	No	Yes	Coinduced with Egr1 on stress[103]	Interacts with heavy metals; stress response[104]
Npw	Neuropeptide W	21.02	8.90E-12	2.26	0.09	np	yes	nr	GPCR ligand; involved in regulating behavior during stress[105]
Nab2	Ngfi-A binding protein 2	13.76	1.50E-101	7.71	0.55	No	Yes	Expression activated by Egr1[92], Egr1 corepressor but also stimulates Egr1-mediated transcription of promoters with few or weak Egr1 sites[61,62]	Transcription factor–negative regulator of Egr1; upregulated by Egr1 as late fibrotic response[57]; promoter has 11 Egr1 sites[106]
Egr1	Early growth response 1; krox24	10.62	2.00E-66	18.07	1.66	Yes	Yes	Egr1 regulates its own promoter[107,108]	Transcription factor that is a key mediator of fibrosis[57]; Egr1 depletion reduces fibrosis[57]
Tagln	Transgelin; Sm22a	9.96	2.20E-46	10.68	1.05	No	No	nr	smooth muscle–specific actin-binding protein; EMT marker[109]
Acta2	Actin, alpha 2, smooth muscle, aorta	9.12	1.60E-48	24.95	2.69	No	Yes	Egr1 coexpressed in SMA positive cells[110], Egr1 can bind to acta2 promoter, represses transcription[111]	Smooth muscle actin; EMT marker in lens[112]
Hmga1-rs1	High-mobility group AT-hook I, related sequence 1; HMGI/Y	7.79	1.70E-24	6.28	0.77	np	No	nr	Upregulated by BMP signaling, drives EMT via SLUG; coexpressed with αSMA and SM22[113]; Binds AT rich DNA in minor groove; regulates chromatin structure
Col26a1	Collagen, type XXVI, alpha 1; emu2	7.44	6.70E-32	2.22	0.29	No	Yes	nr	Collagen variant; expression restricted to mesenchymal cells[114]
Rprm	Reprimo, TP53 dependent G2 arrest mediator candidate	6.9	1.30E-26	5.13	0.72	No	Yes	nr	p53-induced cell cycle arrest gene[115], negative regulator of cell migration, invasion[116]; transiently upregulated during cellular stress[117]

Investigative Ophthalmology & Visual Science

TABLE 3. Continued

Gene ID	Gene Description	Fold Change From WT	FDR, P Value	β1-MLR10 Mean RPKM	WT Mean RPKM	Lens Enrichment iSyTe at E12.5 1.5 Cutoff	Predicted Egr1 Motif in Promoter	Functional Connection With Egr1	Biological Function
Tnfrsf12a	TNF receptor superfamily, member 12a; Tweaker; FN14	4.94	5.20E-17	5.55	1.09	No	Yes	nr	Expression activated by Src[118]; signals via AKT; overexpression in mesenchymal stem cells induces αSMA expression[119]
Itgb8	Integrin beta 8	4.92	9.80E-48	5.9	1.18	No	No	nr	αV integrin binding partner; EMT marker; upregulated during lens EMT[22]; involved in TGFβ activation[120]
Ctss	Cathepsin S	4.89	1.90E-14	2.71	0.53	Yes	No	Coinduced with Egr1 on rabies infection of CNS[121]	Protease secreted at sites of tissue injury and fibrosis, deletion in muscular dystrophy reduces fibrosis[122]; upregulated in Smad4 null hearts leading to aneurysm[123]
Klf4	Kruppel-like factor 4 (gut)	4.85	1.70E-25	2.13	0.43	No	Yes	Egr1 directly binds to the KLF4 promoter and upregulates its expression[83]	Both enhances and inhibits renal fibrosis[124]; upregulates αSMA expression and myofibroblast differentiation in cardiac fibrosis, binds directly to the TGFβ1 promoter[125]; upregulates Pax6 expression in cerebellar granule neuron[126]; activates or represses SM22a expression depending on context[127]; KLF4 deletion from lens results in elevation of ALOX12 (see below, Alox12 is repressed here)[128]
Fos	FBJ osteosarcoma oncogene	4.81	2.50E-11	3.49	0.7	No	No	cFos and Egr1 are both transcriptional targets of STAT[129]; Fos and Egr1 are often coinduced[130]	An early response transcription factor induced in fibrosis[131]

TABLE 3. Continued

Gene ID	Gene Description	Fold Change From WT	FDR, P Value	β1-MLR10 Mean RPKM	WT Mean RPKM	Lens Enrichment iSyTe at E12.5 1.5 Cutoff	Predicted Egr1 Motif in Promoter	Functional Connection With Egr1	Biological Function
Cbac1	ChaC, cation transport regulator 1; glutathione-specific gamma-glutamylcyclotransferase 1;botch	4.57	2.00E-04	4.87	1.08	No	No	nr	Upregulated in UPR in lens[132]; induced by ATF4 during UPR; may be proapoptotic; involved in glutathione degradation[133]
Pak1	p21 protein (Cdc42/Rac)-activated kinase 1	4.23	4.30E-20	2.1	0.49	No	Yes	nr	Upregulated by TGFβ signaling in fibrosis[134]; Key effector of RHO proteins, actin structure; downstream mediator of integrin signaling; regulates FGF23 indirectly[135]
Crip1	Cysteine-rich protein 1 (intestinal)	3.91	1.20E-23	31.41	7.84	No	Yes	Upregulated by Egr1 in Gene Expression Omnibus data[136]	Cytoskeletal protein induced by TGFβ may be involved with fibrosis[137]
Anxa2	Annexin A2	3.81	2.40E-48	24.73	6.35	No	No	Coinduced with Egr1 during neuronal hypoxia[138]	Induced in fibrotic conditions, liver fibrosis marker[38]; involved in regulation of cellular secretion[139]
Mmp2	Matrix metallopeptidase 2	3.55	7.10E-19	2.57	0.72	No	Yes	Egr1 necessary for Mmp2 expression in atherosclerosis[140]; Egr1 binds to the Mmp2 promoter and inhibits its activity[141]	Regulates TGFβ-induced matrix contraction in lens[142], may regulate lens EMT[143]
Fcer1g	Fc receptor, IgE, high affinity I, gamma polypeptide	3.52	2.70E-05	2.5	0.67	No	Yes	nr	Found in immune system, expression activated in CNS by chronic stress[144]
Fas	Fas (TNF receptor superfamily member 6)	3.47	1.20E-17	5.1	1.44	Yes	No	May be upstream of Egr1 induction in fibrosis[145]; Egr1 family members can activate FASI expression/fas pathway[146]	Involved in apoptosis, regulated by TNF[147]; can drive lung fibrosis[145]
C1qa	Complement component 1, q subcomponent, alpha polypeptide	3.47	3.70E-09	3.67	1.02	Yes	No	Co-upregulated with Egr1 during axonal injury[148]	Initiates complement cascade, involved in neural death on stress[149]

Investigative Ophthalmology & Visual Science

TABLE 3. Continued

Gene ID	Gene Description	Fold Change From WT	FDR, P Value	β1-MLR10 Mean RPKM	WT Mean RPKM	Lens Enrichment iSyTe at E12.5 1.5 Cutoff	Predicted Egr1 Motif in Promoter	Functional Connection With Egr1	Biological Function
Plat	Plasminogen activator, tissue	3.31	1.20E-46	9.18	2.71	No	No	nr	Protease; profibrotic factor in vascular injury[150], found at the apical tips of lens epithelial and fiber cells in the embryonic lens[151]
Fgf15	Fibroblast growth factor 15	3.29	3.80E-02	2.31	0.66	No	Yes	nr	Endocrine FGF; requires klothos for its function[152]; fgf15 null mice exhibit less liver fibrosis[153]
Cyr61	Cysteine-rich protein 61 / ccn1	3.27	2.80E-17	3.3	0.99	No	Yes	Egr1 activates cyr61 expression via binding to cyr61 promoter[154]; Egr1 and cyr61 co-upregulated on DNA damage in lens[155], MMP12 null mice downregulate expression of both Egr1 and cyr61[145]	Matricellular protein; can induce EMT/fibrosis[156], may be αVβ5 integrin ligand[157]
Dynlt1b	Dynein light chain Tctex-type 1B	3.24	3.10E-33	57.1	17.19	np	Yes	nr	Molecular motor with role in vesicle transport; binds endoglin and inhibits TGFβ signaling[158]; involved in neural differentiation[159]
Nes	Nestin	3.18	3.60E-68	59.48	18.25	No	Yes	nr	Neurofilament; promotes vimentin disassembly; can be EMT marker[160,161]
S100a13	S100 calcium binding protein A13	3.05	8.90E-05	2.11	0.69	No	No	nr	Involved in RAGE/inflammation[162]
Glipr2	GLI pathogenesis-related 2	3.05	1.70E-29	8.35	2.67	No	Yes	nr	Promotes EMT via Erk activation[163]
Plagl1	Pleiomorphic adenoma gene-like 1; zac1	3	2.40E-18	3.12	1.01	No	Yes	nr	Transcription factor, may regulate TGFβ II expression in retinal development[164]

Investigative Ophthalmology & Visual Science

TABLE 3. Continued

Gene ID	Gene Description	Fold Change From WT	FDR, P Value	β1-MLR10 Mean RPKM	WT Mean RPKM	Lens Enrichment iSyTe at E12.5 1.5 Cutoff	Predicted Egr1 Motif in Promoter	Functional Connection With Egr1	Biological Function
Nab1	Ngfi-A binding protein 1 / EGR binding protein 1	2.99	6.50E-32	4.2	1.38	No	Yes	Corepressor of Egr1, but can also stimulate Egr1 mediated transcription in promoters with few or weak Egr1 sites[62]; Ppromoter has bioinformatically predicted Egr1 site	Might direct myofibroblast de-differentiation[165]; transcriptionally regulated by Pax6 during hind brain development[166]
Emilin1	Elastin microfibril interfacer 1	2.88	4.50E-38	6.44	2.18	No	No	nr	Elastin binding glycoprotein, can negatively regulate TGFβ signaling[167]
Mmp14	Matrix metallopeptidase 14 (membrane-inserted) ; MT1-MMP	2.87	1.30E-34	8.12	2.77	No	Yes	Egr1 directly binds to the MT1-MMP promoter and activates its transcription[84]	Upregulated in kidney fibrosis[168]: may function with αV integrins to activate TGFβ[41], null mice exhibit fibrosis due to lack of collagen turnover[44]
Pbhla3	Pleckstrin homology-like domain, family A, member 3	2.81	1.00E-17	5.97	2.08	No	Yes	nr	Activated on UPR stress[169], inhibits Akt activity by competing for membrane binding sites[170]
Junb	Jun B proto-oncogene	2.8	4.80E-13	3.58	1.27	No	No	Coregulated with Egr1 as IER gene[171,172]	IER TF involved in fibrosis and other stresses[173]
Lgals3	Lectin, galactose binding, soluble 3; galectin3	2.57	2.30E-18	6.22	2.37	No	No	nr	Found in lens fibers, binds MP20[174], carbohydrate binding protein; biomarker of fibrosis in other systems[175]
Gadd45gip1	Growth arrest and DNA-damage-inducible, gamma interacting protein 1 ; crif1	−2.51	5.20E-17	1.97	4.81	No	No	nr	Component of mitoribosome, downregulation is associated with mitochondria dysfunction and ROS production[176]

Investigative Ophthalmology & Visual Science

TABLE 3. Continued

Gene ID	Gene Description	Fold Change From WT	FDR, P Value	β1-MLR10 Mean RPKM	WT Mean RPKM	Lens Enrichment iSyTE at E12.5 1.5 Cutoff	Predicted Egr1 Motif in Promoter	Functional Connection With Egr1	Biological Function
Slc7a11	Solute carrier family 7 (cationic amino acid transporter, y+ system), member 11; Xct	−2.6	6.60E-45	5.46	13.88	Yes	No	nr	Xct deficiency results in autophagy[177]; drives glutamine release during cellular stress[178]; can drive resistance to cellular stress[179]; upregulation of Xct can rescue glutathione deficiency[180]
Tbbs1	Thrombospondin 1	−2.66	1.5E-23	6.89	17.99	No	Yes	Egr1 can bind to thrombospondin promoter directly[181]	Considered to be profibrotic[182]; matricellular protein found at sites of active tissue remodeling in adult eye[183]
Alox12	Arachidonate 12-lipoxygenase	−2.68	3.8E-65	7.35	19.28	Yes	Yes	nr	Produces 12S-HETE that drives inflammation/oxidative stress[184,185], upregulated in KLF4 null lens, KLF4 is activated here, see above[128]
Hmga1	High-mobility group AT-hook 1; HMG-I(Y)	−3.13	7.9E-31	4.18	12.74	nr	Yes	nr	Bends chromatin, recruits TFs to DNA; can be fibrotic marker/regulator[113]
Nnat	Neuronatin; Peg5	−3.46	1.00E-17	1.06	3.7	No	No	nr	Activated on photoreceptor cell stress[186], can regulate calcium signaling[187]

CNS, central nervous system; FDR, false discovery rate; np, gene not represented in the iSyTE data base; nr, none reported.

β1MLR10/Egr1^{−/−} mice are notably larger than those of β1MLR10 animals (Fig. 9B (middle), $n = 7$). Upon dissection, 6 of 7 adult β1MLR10/Egr1^{−/−} eyes contained morphologically identifiable lens tissue (Fig. 9E) that was strongly Aquaporin0 positive (Fig. 9H; $n = 6$).

Because newborn β1MLR10 and β1MLR10/Egr1^{−/−} mouse lenses were of similar size, we then evaluated whether the maintenance of lens material in adult β1MLR10/Egr1^{−/−} lenses (Fig. 8) was due to alterations in apoptosis. As expected, no cleaved Caspase 3 immunoreactivity (Fig. 10A) nor TUNEL-positive nuclei (Fig. 10D) were detected in newborn WT lenses. As previously reported, β1MLR10 lenses exhibited both numerous TUNEL-positive nuclei (Fig. 10E, arrows) and abundant cleaved Caspase 3 (Fig. 10B) staining. Notably, deletion of Egr1 from β1MLR10 mice led to a marked attenuation of cleaved Caspase 3 staining in newborn lenses (Fig. 10C). However, more TUNEL-positive nuclei were detected in β1MLR10/Egr1^{−/−} lens fiber cells (Fig. 10F, arrows) than in β1MLR10 lenses (Fig. 10E, arrows). As low-level Caspase 3 cleavage has been associated with lens fiber cell differentiation,[63,64] we also assessed whether the expression of the Erk responsive fiber cell differentiation regulators, cMaf (Figs. 10G–I) and Prox1 (Figs. 10J–L), was affected by Egr1 deletion from β1MLR10 lenses. Qualitatively, β1MLR10/Egr1^{−/−} LECs stain more intensely for cMaf and Prox1 than β1MLR10 LECs, suggesting that the loss of intense cleaved Caspase 3 staining from β1MLR10/Egr1^{−/−} lenses is not associated with a loss of the aberrant fiber cell differentiation pathway activation previously reported[26] in β1MLR10 lenses.

As the ocular phenotype of adult β1MLR10 mice was less severe in animals that also lacked the *Egr1* gene, we investigated their molecular phenotype at E16.5, the stage at which the first morphological defects are observed in β1MLR10 lenses. As we previously reported,[14] WT E16.5 lenses exhibit high levels β1-integrin immunoreactivity in the lens epithelium and newly elongating cortical fibers, whereas these levels are reduced in the terminally differentiating nuclear fibers (Fig. 11A). In contrast, neither β1MLR10 (Fig. 11B) nor β1MLR10/Egr1^{−/−} (Fig. 11C) lenses exhibit detectable β1-integrin protein, although, in both cases, other ocular structures, including the TVL (arrows), still stain strongly for β1-integrin (Figs. 11B, 11C). We then investigated whether the deletion of *Egr1* altered the pattern of αSMA upregulation in β1MLR10 lenses, as this is the best characterized fibrotic marker in the lens. As previously reported,[26] WT lenses do not exhibit detectable levels of αSMA protein at E16.5 (Fig. 11A; Fig. 11D is αSMA alone), whereas β1MLR10 lenses exhibit obvious αSMA in LECs (Fig. 11B; Fig. 11E is αSMA alone, arrows). This upregulation of αSMA was similar in β1MLR10/Egr1^{−/−} lenses (Fig. 11C; Fig. 11F is αSMA alone, arrows), indicating that Egr1 cannot be the sole driver of αSMA upregulation as a consequence of β1-integrin deletion in the lens. Notably though, although the expression of Nab2 protein was obviously upregulated in β1MLR10 lenses (Fig. 11H) compared with WT (Fig. 11G), no Nab2 protein was detected in β1MLR10/Egr1^{−/−} lenses (Fig. 11I), indicating that Nab2 upregulation is solely under Egr1 control.

DISCUSSION

β1-integrin is localized to the basal surface of all lens cells and is therefore believed to be a regulator of the interactions between lens cells and the lens capsule.[16–18] β1-integrin is also localized to the apical tips and lateral membranes of lens fiber cells where it stabilizes cortical F-actin.[14] In LECs, the function of β1-containing integrins is complex and changes during lens development. Deletion of β1-integrin from the lens vesicle in

β1LE mice leads to defects in lens capsule deposition, as well as in the exit of LECs from the cell cycle, and their differentiation into lens fibers.[15] In contrast, loss of β1-integrin after the completion of primary lens morphogenesis (β1MLR10) leads to a distinct phenotype, wherein LECs initially remain in the cell cycle, but become disorganized, and coexpress the "early" lens fiber cell markers, β-crystallin and cMaf, along with the fibrotic marker αSMA, which is followed by their loss via apoptosis.[26] Here we further our understanding of the molecular basis of this phenotype via gene expression profiling by RNA-seq of mutant lenses, and its partial rescue by deletion of an abnormally upregulated transcriptional regulator.

Deletion of β1-Integrin After the Completion of Initial Lens Morphogenesis Induces Stress Response and Fibrosis-Related Gene Expression
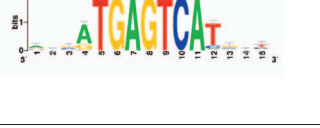
Because the morphological abnormalities of β1MLR10 mouse lenses first become apparent at E16.5, we performed RNA-seq expression profiling on lenses a day earlier, at stage E15.5, to identify molecular changes proximally resulting from β1-integrin deletion, while minimizing the detection of secondary changes. On applying filtering criteria designed to reveal biologically relevant changes in gene expression, 120 DRGs were found. Although several proteins/TFs were found to be altered in β1MLR10 lenses via IF,[26] they were not found to be differentially expressed by RNA-seq. It is likely that either the evaluation of whole lenses masked the subtle changes specifically exhibited by β1MLR10 LECs or the differential protein expression is not controlled at the level of transcription. All the 120 DRGs were prioritized, and analyzed by a variety of bioinformatics tools that use gene ontology databases to identify commonly regulated pathways. However, although "apoptosis," "integrin signaling," and several pathways related to Ras/MapK signaling were identified as relevant, the pathways identified by this method (see Fig. 1) were each based on only a few DRGs, leading us to explore more approaches to gain biological insight into the phenotype.

A comprehensive literature search revealed that nearly half of the 76 upregulated DRGs had known connections to stress response and/or fibrotic pathways. This included αSMA, the most commonly used marker of EMT in the lens,[36,37] which we have previously reported to be upregulated at the protein level in E16.5 β1MLR10 lenses.[26] Validation of four of these genes by qRT-PCR revealed that their mRNA levels are first elevated shortly after loss of β1-integrin protein from the β1MLR10 lens, which is 2 to 3 days earlier than the onset of the obvious lens phenotype.[26] Thus, this induction of stress/fibrotic responses in β1MLR10 mice likely proximately results from the loss of β1-integrin at E12.5 to E13.5. However, although TGF-β is the most intensively studied regulator of EMT and αSMA expression in LECs,[36,65–67] the levels of its downstream regulator, pSmad3, were significantly downregulated in β1MLR10 lenses (Figs. 3A–F) suggesting that TGFβ/Smad signaling is not driving the β1MLR10 phenotype.

β1-Integrin Negatively Regulates Erk1/2 and Akt Signaling in LECs

FAK is expressed in the rodent lens in a pattern similar to β1-integrins,[16,25] and is necessary for fiber cell morphogenesis in zebrafish.[47] Because integrin activation results in the phosphorylation of FAK in other cell types,[49,68] it was not surprising that pFAK (Tyr397) levels are greatly attenuated in β1MLR10 lenses. The loss of pFAK from β1MLR10 lenses is also consistent with the apoptosis observed in newborn β1MLR10

TABLE 4. List of Statistically Overrepresented Motifs (Normalized Enrichment Score ≥3) in the Upstream Region of DRGs

S. No	Enriched Motif ID	Motif Information	NES (Normalized Enriched Score)	Enriched Motif Containing Up- and Down-Regulated DRGs	Motif Logo
1	Factorbook-Egr1	Cys2His2-type	5.78	Ahnak, Alox12, Ankrd34c, Anxa2, Arhgap4, Bcam, Bend6, C1qa, Ccbe1, Ccdc85c, Crabp2, Cyr61, D8Ertd82e, Dctd, Egr1, Emp1, Erbb4, Fgf12, Fgf15, Figla, Fos, Fut10, Gja4, Hmga1, Hmga1-rs1, Hspa8, Itgb8, Junb, Klf4, Ldb2, Mmp14, Nab1,Nab2, Pak1, Paqr7, Phlda3, Plekha2, Ptrf, Rab6b, Rcan2, Rerg, S100a13, Tagln, Thbs1, Tnfrsf12a, Zdhhc2	
2	Swissregulon (SRF) p3	Unknown	5.20	Acta2, Cyr61, Egr1, Fgf15, Fos, Glipr2, Junb, Lgals3, Tagln, Thbs1, Tuft1	
3	Tfdimers-MD00081	Ets domain-family	5.00	Ahnak, Bcam, Ccdc109b, Crabp2, Erbb4, Fcer1g, Hmga1, Hmga1-rs1, Hmgn2, Junb, Nes	
4	Transfac_public-M00490 (V$BACH2_01)	Leucine-zipper	3.10	Bend6, Crabp2, Hmga1, Hmga1-rs1, Htr1d, Klk1b26, Lgals3, Tnfrsf12a	
5	Transfac_public-M00495/V$BACH1_01	Leucine-zipper	3.00	Bend6, Fgf12, Hmga1, Hmga1-rs1, Htr1d, Klk1b26, Lgals3, Plagl1, Tnfrsf12a	

LECs, because pFAK is important for cell survival in other cellular contexts.[68–70] Notably, FAK deletion from fibroblasts leads to the upregulation of αSMA expression,[49] consistent with the upregulation of αSMA expression found β1MLR10 lenses at E16.5.

However, in fibroblasts as well as other cell types, the loss of integrin-mediated FAK phosphorylation often results in a loss of Erk1/2 phosphorylation,[49,71–73] whereas Erk1/2 and Akt phosphorylation are upregulated in both β1MLR10 (this study) and β1LE[15] LECs. There are other precedents for increased Erk and/or Akt activation on integrin deletion, although the proposed mechanisms are diverse. For instance, deletion of emilin1, an α4β1 and α9β1 ligand, from the skin, leads to a downregulation of the phosphatase, PTEN, leading to sustained Erk and Akt phosphorylation.[74] In mesangial cells, α1β1-integrin deletion results in elevated pERK levels due to the ability of this integrin to negatively regulate epidermal growth factor receptor signaling.[75] Thus, it appears likely that β1-integrins can limit Erk/Akt pathway activation in a variety of cellular contexts, including the embryonic lens epithelium.

The IER TF, Egr1, Is Upregulated in β1MLR10 Lenses Shortly After β1-Integrin Loss

Interrogation of the β1MLR10 lens DRGs specifically for TFs regulated by pErk/pAKT activation led to identification of the IER TFs *Egr1*, *Fos*, and *Junb*, all of which were upregulated in these mutant lenses. We focused on *Egr1* because active Erk can elevate Egr1 levels by phosphorylating the Ets-family TF Elk-1[57,59]; *Egr1* is the most upregulated, and most highly expressed, of these three IER genes in E15.5 β1MLR10 lenses; Egr1 can both drive,[76] and make cells resistant to,[77] apoptosis; Egr1 upregulation is first detected coincident with β1-integrin protein loss from both β1MLR10 and β1LE lenses; and the detection of Egr1 protein first in the central lens epithelium, then later in peripheral LECs, correlates with the pattern of LEC loss in the β1MLR10 null lens.

It should be noted that Egr1 mRNA levels remain elevated in the E16.5 β1MLR10 lens, although few Egr1-positive cells were detected at this time by immunolocalization. Although the original reports suggested that Egr1 protein levels are solely controlled at the level of transcription, more recent investigations show that Egr1 protein levels are controlled by microRNA regulation of protein translation[78,79] while Egr1 undergoes extensive posttranslational modifications, including phosphorylation, sumoylation, and acetylation, which affect its stability.[80–82] Thus, it is not surprising that Egr1 protein and mRNA levels do not always correlate.

This upregulation of IER gene expression is likely to be functionally relevant to the β1MLR10 lens phenotype as an unbiased analysis of the 76 upregulated genes revealed that their promoters were enriched in binding motifs for Ets factors,

which are known direct transcriptional effectors of Erk signaling,[55] leucine zipper TFs (like Fos and Junb), and Egr1. This finding suggested that these TFs had the potential to drive the upregulation of many of the DRGs. Further analysis of the DRGs for the presence of Egr1 binding motifs in their putative promoters revealed that 52 of the 120 DRGs had consensus Egr1 binding sites in the 2.5 kb of sequence upstream of their TSS. Notably, eight of these promoters are already known to be directly regulated by Egr1 (Table 3). For example, Egr1 directly binds to and upregulates expression driven by the promoter of the Kruppel-related TF, *Klf4*, in HepG2 cells.[83] Egr1 also directly binds to and upregulates the expression of *MMP14*, a gene encoding MT1-MMP, a matrix metalloprotease that can activate latent TGF-β.[84] Similarly, Egr1 activates the expression of the most upregulated TF in the E15.5 β1MLR10 lens, Nab2, which is best known for its ability to heterodimerize with Egr1, acting as an Egr1 corepressor.[85–87] Notably, Nab2 upregulation driven by Egr1 blocks the ability of Egr1 to upregulate its own expression, limiting the IER.[57,86] This negative feedback loop likely explains why Nab2 protein upregulation persists in β1-integrin null lens cells longer than Egr1.

However, Nab2-Egr1 interactions also can stimulate gene expression driven by promoters harboring weak Egr1 binding sites.[61] This functional complexity may explain the observation that consensus Egr1 binding sites were identified in the promoters of both upregulated ($n = 31$) and downregulated ($n = 21$) DRGs. Overall, this analysis suggests that the upregulation of Egr1 may participate in both the positive and negative regulation of β1MLR10 DRGs.

Elevated Egr1 Expression in β1MLR10 LECs Causes a Subset of the β1MLR10 Lens Phenotype

In the eye, Egr1 mediates the connection between image focus on the retina and eye growth, and Egr1 null mice develop myopia associated with elevated growth of the sclera and changes in lens optics.[88] In the lens, Egr1 expression is upregulated during cellular stresses such as selenite treatment,[89] whereas knockdown of Egr1 in cultured LECs can attenuate selenite-induced cell death.[90] Thus, we generated β1MLR10/Egr1$^{-/-}$ mice to evaluate the extent to which the β1MLR10 lens phenotype was a consequence of Egr1 upregulation. Notably, deletion of the Egr1 gene partially rescued the microphthalmia seen in β1MLR10 adults. This partial rescue is likely related to the observed attenuation of Caspase 3 cleavage in perinatal β1MLR10/Egr1$^{-/-}$ lenses, leading to enhanced cell survival of the lens epithelium compared with β1MLR10 lenses. However, it should be noted that β1MLR10/Egr1$^{-/-}$ lenses are still TUNEL positive, particularly within the lens fibers, suggesting that either multiple cell death pathways are active in β1MLR10 lenses, or that Egr1 is able to simultaneously influence prosurvival and proapoptotic pathways in the lens. Alternatively, as β1MLR10 lenses lacking Egr1 appear to upregulate the Erk responsive TFs cMaf[91] and Prox1,[29] Egr1 upregulation in β1-integrin null LECs may limit the ability of these cells to enter the fiber cell differentiation pathway.

Another major feature of β1MLR10 lenses is the upregulation of the "fibrotic" marker, αSMA, in LECs. However, Egr1 expression is also found to be upregulated in the β1LE lens, which does not exhibit upregulation of αSMA,[15] and we find that deletion of Egr1 from the β1MLR10 lens did not noticeably affect the upregulation of αSMA. However, Egr1 appears to directly control the expression of Nab2 in the lens. First, although both Egr1 and Nab2 mRNA and protein levels are upregulated in β1MLR10 lenses proximal to the loss of β1-integrin protein, Nab2 upregulation lags behind that of Egr1. Second, Nab2 protein expression is not upregulated in β1MLR10 lenses lacking Egr1, whereas Nab2 is highly upregulated in β1MLR10 LECs. These observations are consistent with the known ability of Egr1 to bind to the Nab2 promoter, activating Nab2 expression, which subsequently downregulates Egr1 expression, limiting the IER.[92] The possibility that Egr1 is generally induced in the lens in response to cellular stress, and the role its induction plays in mediating cellular stress responses, is a fruitful topic of future study.

Conclusions

β1-integrin deletion from the lens after the completion of its primary morphogenesis (β1MLR10) leads to activation of Erk/Akt signaling, upregulation of IER genes, as well as numerous markers of cellular stress. As Egr1 expression is also elevated in lenses undergoing stress postnatally,[90,93] and deletion of Egr1 from β1MLR10 lenses attenuates part of the phenotype, the role of Egr1 in mediating stress responses in the lens epithelium represents a novel finding worthy of further investigation.

References

1. Zampighi GA, Eskandari S, Kreman M. Epithelial organization of the mammalian lens. *Exp Eye Res*. 2000;71:415–435.
2. Bassnett S, Shi Y, Vrensen GF. Biological glass: structural determinants of eye lens transparency. *Philos Trans R Soc Lond B Biol Sci*. 2011;366:1250–1264.
3. Danysh BP, Duncan MK. The lens capsule. *Exp Eye Res*. 2009;88:151–164.
4. Mathias RT, Kistler J, Donaldson P. The lens circulation. *J Membr Biol*. 2007;216:1–16.
5. Joy A, Al-Ghoul KJ. Basal membrane complex architecture is disrupted during posterior subcapsular cataract formation in Royal College of Surgeons rats. *Mol Vis*. 2014;20:1777–1795.
6. Sindhu Kumari S, Varadaraj K. Intact and N- or C-terminal end truncated AQP0 function as open water channels and cell-to-cell adhesion proteins: end truncation could be a prelude for adjusting the refractive index of the lens to prevent spherical aberration. *Biochim Biophys Acta*. 2014;1840:2862–2877.
7. Zelenka PS. Regulation of cell adhesion and migration in lens development. *Int J Dev Biol*. 2004;48:857–865.
8. Wang Z, Schey KL. Proteomic analysis of lipid raft-like detergent-resistant membranes of lens fiber cells. *Invest Ophthalmol Vis Sci*. 2015;56:8349–8360.
9. Wang Z, Han J, David LL, Schey KL. Proteomics and phosphoproteomics analysis of human lens fiber cell membranes. *Invest Ophthalmol Vis Sci*. 2013;54:1135–1143.
10. Hynes RO. Integrins: bidirectional, allosteric signaling machines. *Cell*. 2002;110:673–687.

11. Hynes RO. Integrins: a family of cell surface receptors. *Cell*. 1987;48:549–554.

12. Longhurst CM, Jennings LK. Integrin-mediated signal transduction. *Cell Mol Life Sci*. 1998;54:514–526.

13. Menko AS, Philip NJ. Beta 1 integrins in epithelial tissues: a unique distribution in the lens. *Exp Cell Res*. 1995;218:516–521.

14. Scheiblin DA, Gao J, Caplan JL, et al. Beta-1 integrin is important for the structural maintenance and homeostasis of differentiating fiber cells. *Int J Biochem Cell Biol*. 2014;50:132–145.

15. Pathania M, Wang Y, Simirskii VN, Duncan MK. β1-integrin controls cell fate specification in early lens development. *Differentiation*. 2016;92:133–147.

16. Bassnett S, Missey H, Vucemilo I. Molecular architecture of the lens fiber cell basal membrane complex. *J Cell Sci*. 1999;112:2155–2165.

17. Zhang Y, Fan J, Ho JW, et al. Crim1 regulates integrin signaling in murine lens development. *Development*. 2016;143:356–366.

18. Cammas L, Wolfe J, Choi SY, Dedhar S, Beggs HE. Integrin-linked kinase deletion in the developing lens leads to capsule rupture, impaired fiber migration and non-apoptotic epithelial cell death. *Invest Ophthalmol Vis Sci*. 2012;53:3067–3081.

19. Manthey AL, Lachke SA, FitzGerald PG, et al. Loss of Sip1 leads to migration defects and retention of ectodermal markers during lens development. *Mech Dev*. 2014;131:86–110.

20. De Arcangelis A, Mark M, Kreidberg J, Sorokin L, Georges-Labouesse E. Synergistic activities of alpha3 and alpha6 integrins are required during apical ectodermal ridge formation and organogenesis in the mouse. *Development*. 1999;126:3957–3968.

21. Basu S, Rajakaruna S, De Arcangelis A, Zhang L, Georges-Labouesse E, Menko AS. α6 integrin transactivates insulin-like growth factor receptor-1 (IGF-1R) to regulate caspase-3-mediated lens epithelial cell differentiation initiation. *J Biol Chem*. 2014;289:3842–3855.

22. Mamuya FA, Wang Y, Roop VH, Scheiblin DA, Zajac JC, Duncan MK. The roles of αV integrins in lens EMT and posterior capsular opacification. *J Cell Mol Med*. 2014;18:656–670.

23. Walker JL, Zhang L, Menko AS. A signaling role for the uncleaved form of alpha 6 integrin in differentiating lens fiber cells. *Dev Biol*. 2002;251:195–205.

24. Walker JL, Zhang L, Zhou J, Woolkalis MJ, Menko AS. Role for alpha 6 integrin during lens development: evidence for signaling through IGF-1R and ERK. *Dev Dyn*. 2002;223:273–284.

25. Kokkinos MI, Brown HJ, de Iongh RU. Focal adhesion kinase (FAK) expression and activation during lens development. *Mol Vis*. 2007;13:418–430.

26. Simirskii VN, Wang Y, Duncan MK. Conditional deletion of beta1-integrin from the developing lens leads to loss of the lens epithelial phenotype. *Dev Biol*. 2007;306:658–668.

27. Lee SL, Tourtellotte LC, Wesselschmidt RL, Milbrandt J. Growth and differentiation proceeds normally in cells deficient in the immediate early gene NGFI-A. *J Biol Chem*. 1995;270:9971–9977.

28. Manthey AL, Terrell AM, Lachke SA, Polson SW, Duncan MK. Development of novel filtering criteria to analyze RNA-sequencing data obtained from the murine ocular lens during embryogenesis. *Genom Data*. 2014;2:369–374.

29. Audette DS, Anand D, So T, et al. Prox1 and fibroblast growth factor receptors form a novel regulatory loop controlling lens fiber differentiation and gene expression. *Development*. 2016;143:318–328.

30. Mi H, Poudel S, Muruganujan A, Casagrande JT, Thomas PD. PANTHER version 10: expanded protein families and functions, and analysis tools. *Nucleic Acids Res*. 2016;44:D336–D342.

31. Lachke SA, Ho JW, Kryukov GV, et al. iSyTE: integrated Systems Tool for Eye gene discovery. *Invest Ophthalmol Vis Sci*. 2012;53:1617–1627.

32. Janky R, Verfaillie A, Imrichová H, et al. iRegulon: from a gene list to a gene regulatory network using large motif and track collections. *PLoS Comput Biol*. 2014;10:e1003731.

33. Mathelier A, Zhao X, Zhang AW, et al. JASPAR 2014: an extensively expanded and updated open-access database of transcription factor binding profiles. *Nucleic Acids Res*. 2014;42:D142–D147.

34. Reed NA, Oh DJ, Czymmek KJ, Duncan MK. An immunohistochemical method for the detection of proteins in the vertebrate lens. *J Immunol Methods*. 2001;253:243–252.

35. Anand D, Lachke SA. Systems biology of lens development: a paradigm for disease gene discovery in the eye. *Exp Eye Res*. 2017;156:22–33.

36. de Iongh RU, Wederell E, Lovicu FJ, McAvoy JW. Transforming growth factor-beta-induced epithelial-mesenchymal transition in the lens: a model for cataract formation. *Cells Tissues Organs*. 2005;179:43–55.

37. Garcia CM, Kwon GP, Beebe DC. alpha-Smooth muscle actin is constitutively expressed in the lens epithelial cells of several species. *Exp Eye Res*. 2006;83:999–1001.

38. Zhang L, Peng X, Zhang Z, et al. Subcellular proteome analysis unraveled annexin A2 related to immune liver fibrosis. *J Cell Biochem*. 2010;110:219–228.

39. Muimo R. Regulation of CFTR function by annexin A2-S100A10 complex in health and disease. *Gen Physiol Biophys*. 2009;28:F14–F19.

40. Truter SL, Dumlao TF, Lee JA, Lee E, Supino PG, Borer JS. Vesnarinone-mediated alterations of gene expression in cardiac fibroblasts from aortic regurgitant hearts. *Am J Ther*. 2004;11:328–336.

41. Robertson IB, Rifkin DB. Unchaining the beast; insights from structural and evolutionary studies on TGFβ secretion, sequestration, and activation. *Cytokine Growth Factor Rev*. 2013;24:355–372.

42. Hemmann S, Graf J, Roderfeld M, Roeb E. Expression of MMPs and TIMPs in liver fibrosis—a systematic review with special emphasis on anti-fibrotic strategies. *J Hepatol*. 2007;46:955–975.

43. Iredale JP. Models of liver fibrosis: exploring the dynamic nature of inflammation and repair in a solid organ. *J Clin Invest*. 2007;117:539–548.

44. Holmbeck K, Bianco P, Caterina J, et al. MT1-MMP-deficient mice develop dwarfism, osteopenia, arthritis, and connective tissue disease due to inadequate collagen turnover. *Cell*. 1999;99:81–92.

45. Ghosh AK, Vaughan DE. PAI-1 in tissue fibrosis. *J Cell Physiol*. 2012;227:493–507.

46. Kaminski N, Rosas IO. Gene expression profiling as a window into idiopathic pulmonary fibrosis pathogenesis: can we identify the right target genes? *Proc Am Thorac Soc*. 2006;3:339–344.

47. Hayes JM, Hartsock A, Clark BS, Napier HR, Link BA, Gross JM. Integrin α5/fibronectin1 and focal adhesion kinase are required for lens fiber morphogenesis in zebrafish. *Mol Biol Cell*. 2012;23:4725–4738.

48. Ding Q, Gladson CL, Wu H, Hayasaka H, Olman MA. Focal adhesion kinase (FAK)-related non-kinase inhibits myofibroblast differentiation through differential MAPK activation in a FAK-dependent manner. *J Biol Chem*. 2008;283:26839–26849.

49. Greenberg RS, Bernstein AM, Benezra M, Gelman IH, Taliana L, Masur SK. FAK-dependent regulation of myofibroblast differentiation. *FASEB J*. 2006;20:1006–1008.

50. Lovicu FJ, McAvoy JW. FGF-induced lens cell proliferation and differentiation is dependent on MAPK (ERK1/2) signalling. *Development*. 2001;128:5075–5084.

51. Iyengar L, Wang Q, Rasko JE, McAvoy JW, Lovicu FJ. Duration of ERK1/2 phosphorylation induced by FGF or ocular media determines lens cell fate. *Differentiation*. 2007;75:662–668.

52. Tullai JW, Schaffer ME, Mullenbrock S, Sholder G, Kasif S, Cooper GM. Immediate-early and delayed primary response genes are distinct in function and genomic architecture. *J Biol Chem*. 2007;282:23981–23995.

53. O'Donnell A, Odrowaz Z, Sharrocks AD. Immediate-early gene activation by the MAPK pathways: what do and don't we know? *Biochem Soc Trans*. 2012;40:58–66.

54. Murphy LO, MacKeigan JP, Blenis J. A network of immediate early gene products propagates subtle differences in mitogen-activated protein kinase signal amplitude and duration. *Mol Cell Biol*. 2004;24:144–153.

55. Roskoski R Jr. ERK1/2 MAP kinases: structure, function, and regulation. *Pharmacol Res*. 2012;66:105–143.

56. Gitenay D, Baron VT. Is EGR1 a potential target for prostate cancer therapy? *Future Oncol*. 2009;5:993–1003.

57. Bhattacharyya S, Wu M, Fang F, Tourtellotte W, Feghali-Bostwick C, Varga J. Early growth response transcription factors: key mediators of fibrosis and novel targets for anti-fibrotic therapy. *Matrix Biol*. 2011;30:235–242.

58. Bhattacharyya S, Fang F, Tourtellotte W, Varga J. Egr-1: new conductor for the tissue repair orchestra directs harmony (regeneration) or cacophony (fibrosis). *J Pathol*. 2013;229:286–297.

59. Pagel JI, Deindl E. Early growth response 1—a transcription factor in the crossfire of signal transduction cascades. *Indian J Biochem Biophys*. 2011;48:226–235.

60. Tur G, Georgieva EI, Gagete A, Lopez-Rodas G, Rodriguez JL, Franco L. Factor binding and chromatin modification in the promoter of murine Egr1 gene upon induction. *Cell Mol Life Sci*. 2010;67:4065–4077.

61. Collins S, Wolfraim LA, Drake CG, Horton MR, Powell JD. Cutting edge: TCR-induced NAB2 enhances T cell function by coactivating IL-2 transcription. *J Immunol*. 2006;177:8301–8305.

62. Sevetson BR, Svaren J, Milbrandt J. A novel activation function for NAB proteins in EGR-dependent transcription of the luteinizing hormone beta gene. *J Biol Chem*. 2000;275:9749–9757.

63. Weber GF, Menko AS. The canonical intrinsic mitochondrial death pathway has a non-apoptotic role in signaling lens cell differentiation. *J Biol Chem*. 2005;280:22135–22145.

64. Zandy AJ, Lakhani S, Zheng T, Flavell RA, Bassnett S. Role of the executioner caspases during lens development. *J Biol Chem*. 2005;280:30263–30272.

65. St-Onge L, Sosa-Pineda B, Chowdhury K, Mansouri A, Gruss P. Pax6 is required for differentiation of glucagon-producing alpha-cells in mouse pancreas. *Nature*. 1997;387:406–409.

66. Hu B, Wu Z, Phan SH. Smad3 mediates transforming growth factor-beta-induced alpha-smooth muscle actin expression. *Am J Respir Cell Mol Biol*. 2003;29:397–404.

67. Zavadil J, Bottinger EP. TGF-beta and epithelial-to-mesenchymal transitions. *Oncogene*. 2005;24:5764–5774.

68. Hakuno D, Takahashi T, Lammerding J, Lee RT. Focal adhesion kinase signaling regulates cardiogenesis of embryonic stem cells. *J Biol Chem*. 2005;280:39534–39544.

69. Schaller MD. Biochemical signals and biological responses elicited by the focal adhesion kinase. *Biochim Biophys Acta*. 2001;1540:1–21.

70. Mitra SK, Hanson DA, Schlaepfer DD. Focal adhesion kinase: in command and control of cell motility. *Nat Rev Mol Cell Biol*. 2005;6:56–68.

71. Lee DY, Li YS, Chang SF, et al. Oscillatory flow-induced proliferation of osteoblast-like cells is mediated by alphavbeta3 and beta1 integrins through synergistic interactions of focal adhesion kinase and Shc with phosphatidylinositol 3-kinase and the Akt/mTOR/p70S6K pathway. *J Biol Chem*. 2010;285:30–42.

72. Cabodi S, Morello V, Masi A, et al. Convergence of integrins and EGF receptor signaling via PI3K/Akt/FoxO pathway in early gene Egr-1 expression. *J Cell Physiol*. 2009;218:294–303.

73. Riopel M, Krishnamurthy M, Li J, Liu S, Leask A, Wang R. Conditional β1-integrin-deficient mice display impaired pancreatic β cell function. *J Pathol*. 2011;224:45–55.

74. Danussi C, Petrucco A, Wassermann B, et al. EMILIN1-α4/α9 integrin interaction inhibits dermal fibroblast and keratinocyte proliferation. *J Cell Biol*. 2011;195:131–145.

75. Chen X, Whiting C, Borza C, et al. Integrin alpha1beta1 regulates epidermal growth factor receptor activation by controlling peroxisome proliferator-activated receptor gamma-dependent caveolin-1 expression. *Mol Cell Biol*. 2010;30:3048–3058.

76. Virolle T, Adamson ED, Baron V, et al. The Egr-1 transcription factor directly activates PTEN during irradiation-induced signalling. *Nat Cell Biol*. 2001;3:1124–1128.

77. Lee CG, Cho SJ, Kang MJ, et al. Early growth response gene 1-mediated apoptosis is essential for transforming growth factor beta1-induced pulmonary fibrosis. *J Exp Med*. 2004;200:377–389.

78. Li Y, McRobb LS, Khachigian LM. MicroRNA miR-191 targets the zinc finger transcription factor Egr-1 and suppresses intimal thickening after carotid injury. *Int J Cardiol*. 2016;212:299–302.

79. Wu SY, Rupaimoole R, Shen F, et al. A miR-192-EGR1-HOXB9 regulatory network controls the angiogenic switch in cancer. *Nat Commun*. 2016;7:11169.

80. Vedantham S, Thiagarajan D, Ananthakrishnan R, et al. Aldose reductase drives hyperacetylation of Egr-1 in hyperglycemia and consequent upregulation of proinflammatory and prothrombotic signals. *Diabetes*. 2014;63:761–774.

81. Cao X, Mahendran R, Guy GR, Tan YH. Protein phosphatase inhibitors induce the sustained expression of the Egr-1 gene and the hyperphosphorylation of its gene product. *J Biol Chem*. 1992;267:12991–12997.

82. Manente AG, Pinton G, Tavian D, Lopez-Rodas G, Brunelli E, Moro L. Coordinated sumoylation and ubiquitination modulate EGF induced EGR1 expression and stability. *PLoS One*. 2011;6:e25676.

83. Lai JK, Wu HC, Shen YC, Hsieh HY, Yang SY, Chang CC. Krüppel-like factor 4 is involved in cell scattering induced by hepatocyte growth factor. *J Cell Sci*. 2012;125:4853–4864.

84. Haas TL, Stitelman D, Davis SJ, Apte SS, Madri JA. Egr-1 mediates extracellular matrix-driven transcription of membrane type 1 matrix metalloproteinase in endothelium. *J Biol Chem*. 1999;274:22679–22685.

85. Srinivasan R, Mager GM, Ward RM, Mayer J, Svaren J. NAB2 represses transcription by interacting with the CHD4 subunit of the nucleosome remodeling and deacetylase (NuRD) complex. *J Biol Chem*. 2006;281:15129–15137.

86. Ehrengruber MU, Muhlebach SG, Söhrman S, Leutenegger CM, Lester HA, Davidson N. Modulation of early growth response (EGR) transcription factor-dependent gene expression by using recombinant adenovirus. *Gene*. 2000;258:63–69.

87. Russo MW, Sevetson BR, Milbrandt J. Identification of NAB1, a repressor of NGFI-A- and Krox20-mediated transcription. *Proc Natl Acad Sci U S A*. 1995;92:6873–6877.

88. Schippert R, Burkhardt E, Feldkaemper M, Schaeffel F. Relative axial myopia in Egr-1 (ZENK) knockout mice. *Invest Ophthalmol Vis Sci*. 2007;48:11–17.

89. Belusko PB, Nakajima T, Azuma M, Shearer TR. Expression changes in mRNAs and mitochondrial damage in lens epithelial cells with selenite. *Biochim Biophys Acta* 2003; 1623:135–142.

90. Nakajima T, Belusko PB, Walkup RD, Azuma M, Shearer TR. Involvement of Egr-1 in lens epithelial cell death induced by selenite. *Exp Eye Res*. 2006;82:874–878.

91. Xie Q, McGreal R, Harris R, et al. Regulation of c-Maf and αA-crystallin in ocular lens by fibroblast growth factor signaling. *J Biol Chem*. 2016;291:3947–3958.

92. Kumbrink J, Kirsch KH, Johnson JP. EGR1, EGR2, and EGR3 activate the expression of their coregulator NAB2 establishing a negative feedback loop in cells of neuroectodermal and epithelial origin. *J Cell Biochem*. 2010;111:207–217.

93. Paron I, D'Elia A, D'Ambrosio C, et al. A proteomic approach to identify early molecular targets of oxidative stress in human epithelial lens cells. *Biochem J*. 2004;378:929–937.

94. Zhao H, Yang Y, Rizo CM, Overbeek PA, Robinson ML. Insertion of a Pax6 consensus binding site into the alphaA-crystallin promoter acts as a lens epithelial cell enhancer in transgenic mice. *Invest Ophthalmol Vis Sci*. 2004;45:1930–1939.

95. Bhattacharyya S, Wei J, Melichian DS, Milbrandt J, Takehara K, Varga J. The transcriptional cofactor nab2 is induced by tgf-Beta and suppresses fibroblast activation: physiological roles and impaired expression in scleroderma. *PLoS One*. 2009;4:e7620.

96. Pankhurst MW, Bennett W, Kirkcaldie MT, West AK, Chung RS. Increased circulating leukocyte numbers and altered macrophage phenotype correlate with the altered immune response to brain injury in metallothionein (MT)-I/II null mutant mice. *J Neuroinflammation*. 2011;8:172.

97. Huang B, Deora AB, He KL, et al. Hypoxia-inducible factor-1 drives annexin A2 system-mediated perivascular fibrin clearance in oxygen-induced retinopathy in mice. *Blood*. 2011;118:2918–2929.

98. Hayashi H, Sakai K, Baba H, Sakai T. Thrombospondin-1 is a novel negative regulator of liver regeneration after partial hepatectomy through transforming growth factor-beta1 activation in mice. *Hepatology*. 2012;55:1562–1573.

99. Martel G, Hevi C, Wong A, Zushida K, Uchida S, Shumyatsky GP. Murine GRPR and stathmin control in opposite directions both cued fear extinction and neural activities of the amygdala and prefrontal cortex. *PLoS One*. 2012;7: e30942.

100. Fowler JC, Zecchini VR, Jones PH. Intestinal activation of Notch signaling induces rapid onset hepatic steatosis and insulin resistance. *PLoS One*. 2011;6:e20767.

101. Borgo C, Franchin C, Salizzato V, et al. Protein kinase CK2 potentiates translation efficiency by phosphorylating eIF3j at Ser127. *Biochim Biophys Acta*. 2015;1853:1693–1701.

102. Chiu WL, Wagner S, Herrmannová A, et al. The C-terminal region of eukaryotic translation initiation factor 3a (eIF3a) promotes mRNA recruitment, scanning, and, together with eIF3j and the eIF3b RNA recognition motif, selection of AUG start codons. *Mol Cell Biol*. 2010;30:4415–4434.

103. Liu J, Zhou ZX, Zhang W, Bell MW, Waalkes MP. Changes in hepatic gene expression in response to hepatoprotective levels of zinc. *Liver Int*. 2009;29:1222–1229.

104. Takahashi S. Positive and negative regulators of the metallothionein gene (review). *Mol Med Rep*. 2015;12: 795–799.

105. Motoike T, Long JM, Tanaka H, et al. Mesolimbic neuropeptide W coordinates stress responses under novel environments. *Proc Natl Acad Sci U S A*. 2016;113:6023–6028.

106. Kumbrink J, Gerlinger M, Johnson JP. Egr-1 induces the expression of its corepressor nab2 by activation of the nab2 promoter thereby establishing a negative feedback loop. *J Biol Chem*. 2005;280:42785–42793.

107. Cao X, Mahendran R, Guy GR, Tan YH. Detection and characterization of cellular EGR-1 binding to its recognition site. *J Biol Chem*. 1993;268:16949–16957.

108. Wang B, Chen J, Santiago FS, et al. Phosphorylation and acetylation of histone H3 and autoregulation by early growth response 1 mediate interleukin 1beta induction of early growth response 1 transcription. *Arterioscler Thromb Vasc Biol*. 2010;30:536–545.

109. Dong LH, Lv P, Han M. Roles of SM22α in cellular plasticity and vascular diseases. *Cardiovasc Hematol Disord Drug Targets*. 2012;12:119–125.

110. McCaffrey TA, Fu C, Du B, et al. High-level expression of Egr-1 and Egr-1-inducible genes in mouse and human atherosclerosis. *J Clin Invest*. 2000;105:653–662.

111. Liu X, Kelm RJ, Strauch AR. Transforming growth factor beta1-mediated activation of the smooth muscle alpha-actin gene in human pulmonary myofibroblasts is inhibited by tumor necrosis factor-alpha via mitogen-activated protein kinase kinase 1-dependent induction of the Egr-1 transcriptional repressor. *Mol Biol Cell*. 2009;20:2174–2185.

112. Manthey AL, Terrell AM, Wang Y, Taube JR, Yallowitz AR, Duncan MK. The Zeb proteins δEF1 and Sip1 may have distinct functions in lens cells following cataract surgery. *Invest Ophthalmol Vis Sci*. 2014;55:5445–5455.

113. Hopper RK, Moonen JR, Diebold I, et al. In pulmonary arterial hypertension, reduced BMPR2 promotes endothelial-to-mesenchymal transition via HMGA1 and its target slug. *Circulation*. 2016;133:1783–1794.

114. Leimeister C, Steidl C, Schumacher N, Erhard S, Gessler M. Developmental expression and biochemical characterization of Emu family members. *Dev Biol*. 2002;249:204–218.

115. Ohki R, Nemoto J, Murasawa H, et al. Reprimo, a new candidate mediator of the p53-mediated cell cycle arrest at the G2 phase. *J Biol Chem*. 2000;275:22627–22630.

116. Buchegger K, Ili C, Riquelme I, et al. Reprimo as a modulator of cell migration and invasion in the MDA-MB-231 breast cancer cell line. *Biol Res*. 2016;49:5.

117. Xu M, Knox AJ, Michaelis KA, et al. Reprimo (RPRM) is a novel tumor suppressor in pituitary tumors and regulates survival, proliferation, and tumorigenicity. *Endocrinology*. 2012;153:2963–2973.

118. Cheng E, Whitsett TG, Tran NL, Winkles JA. The TWEAK receptor Fn14 is an Src-inducible protein and a positive regulator of Src-driven cell invasion. *Mol Cancer Res*. 2015; 13:575–583.

119. So T, Croft M. Regulation of PI-3-kinase and Akt signaling in T lymphocytes and other cells by TNFR family molecules. *Front Immunol*. 2013;4:139.

120. Kumar V, Maurya VK, Joshi A, Meeran SM, Jha RK. Integrin beta 8 (ITGB8) regulates embryo implantation potentially via controlling the activity of TGF-B1 in mice. *Biol Reprod*. 2015;92:109.

121. Saha S, Rangarajan PN. Common host genes are activated in mouse brain by Japanese encephalitis and rabies viruses. *J Gen Virol*. 2003;84:1729–1735.

122. Tjondrokoesoemo A, Schips TG, Sargent MA, et al. Cathepsin S contributes to the pathogenesis of muscular dystrophy in mice. *J Biol Chem*. 2016;291:9920–9928.

123. Zhang P, Hou S, Chen J, et al. Smad4 deficiency in smooth muscle cells initiates the formation of aortic aneurysm. *Circ Res*. 2016;118:388–399.

124. Ke B, Zhang A, Wu X, Fang X. The role of Krüppel-like factor 4 in renal fibrosis. *Front Physiol*. 2015;6:327.

125. Zhang Y, Wang Y, Liu Y, Wang N, Qi Y, Du J. Krüppel-like factor 4 transcriptionally regulates TGF-β1 and contributes to cardiac myofibroblast differentiation. *PLoS One*. 2013;8: e63424.

126. Zhang P, Ha T, Larouche M, Swanson D, Goldowitz D. Kruppel-like factor 4 regulates granule cell Pax6 expression and cell proliferation in early cerebellar development. *PLoS One*. 2015;10:e0134390.

127. Yu K, Zheng B, Han M, Wen JK. ATRA activates and PDGF-BB represses the SM22α promoter through KLF4 binding to, or dissociating from, its cis-DNA elements. *Cardiovasc Res*. 2011;90:464–474.

128. Gupta D, Harvey SA, Kenchegowda D, Swamynathan S, Swamynathan SK. Regulation of mouse lens maturation and gene expression by Krüppel-like factor 4. *Exp Eye Res*. 2013; 116:205–218.

129. Schiavone D, Avalle L, Dewilde S, Poli V. The immediate early genes Fos and Egr1 become STAT1 transcriptional targets in the absence of STAT3. *FEBS Lett*. 2011;585:2455–2460.

130. Madabhushi R, Gao F, Pfenning AR, et al. Activity-induced DNA breaks govern the expression of neuronal early-response genes. *Cell*. 2015;161:1592–1605.

131. Robledo R, Mossman B. Cellular and molecular mechanisms of asbestos-induced fibrosis. *J Cell Physiol*. 1999;180:158–166.

132. Zhou Y, Bennett TM, Shiels A. Lens ER-stress response during cataract development in Mip-mutant mice. *Biochim Biophys Acta*. 2016;1862:1433–1442.

133. Crawford RR, Prescott ET, Sylvester CF, et al. Human CHAC1 protein degrades glutathione, and mRNA induction is regulated by the transcription factors ATF4 and ATF3 and a bipartite ATF/CRE regulatory element. *J Biol Chem*. 2015; 290:15878–15891.

134. Chen G, Chen X, Sukumar A, et al. TGFβ receptor I transactivation mediates stretch-induced Pak1 activation and CTGF upregulation in mesangial cells. *J Cell Sci*. 2013; 126:3697–3712.

135. Fajol A, Honisch S, Zhang B, et al. Fibroblast growth factor (Fgf) 23 gene transcription depends on actin cytoskeleton reorganization. *FEBS Lett*. 2016;590:705–715.

136. Hu H, Zhou DS, Yu R. Effects of compound danshen tablet on the expression of Abeta in transgenic cell model of Alzheimer's disease [in Chinese]. *Zhongguo Zhong Xi Yi Jie He Za Zhi*. 2012;32:1663–1666.

137. Järvinen PM, Myllärniemi M, Liu H, et al. Cysteine-rich protein 1 is regulated by transforming growth factor-β1 and expressed in lung fibrosis. *J Cell Physiol*. 2012;227:2605–2612.

138. Jin K, Mao XO, Eshoo MW, et al. cDNA microarray analysis of changes in gene expression induced by neuronal hypoxia in vitro. *Neurochem Res*. 2002;27:1105–1112.

139. Gabel M, Delavoie F, Demais V, et al. Annexin A2-dependent actin bundling promotes secretory granule docking to the plasma membrane and exocytosis. *J Cell Biol*. 2015;210: 785–800.

140. Harja E, Chang JS, Lu Y, et al. Mice deficient in PKCbeta and apolipoprotein E display decreased atherosclerosis. *FASEB J*. 2009;23:1081–1091.

141. Zcharia E, Atzmon R, Nagler A, et al. Inhibition of matrix metalloproteinase-2 by halofuginone is mediated by the Egr1 transcription factor. *Anticancer Drugs*. 2012;23:1022–1031.

142. Eldred JA, Hodgkinson LM, Dawes LJ, Reddan JR, Edwards DR, Wormstone IM. MMP2 activity is critical for TGFβ2-induced matrix contraction—implications for fibrosis. *Invest Ophthalmol Vis Sci*. 2012;53:4085–4098.

143. Awasthi N, Wang-Su ST, Wagner BJ. Downregulation of MMP-2 and -9 by proteasome inhibition: a possible mechanism to decrease LEC migration and prevent posterior capsular opacification. *Invest Ophthalmol Vis Sci*. 2008;49:1998–2003.

144. Lisowski P, Wieczorek M, Goscik J, et al. Effects of chronic stress on prefrontal cortex transcriptome in mice displaying different genetic backgrounds. *J Mol Neurosci*. 2013;50:33–57.

145. Matute-Bello G, Wurfel MM, Lee JS, et al. Essential role of MMP-12 in Fas-induced lung fibrosis. *Am J Respir Cell Mol Biol*. 2007;37:210–221.

146. Droin NM, Pinkoski MJ, Dejardin E, Green DR. Egr family members regulate nonlymphoid expression of Fas ligand, TRAIL, and tumor necrosis factor during immune responses. *Mol Cell Biol*. 2003;23:7638–7647.

147. Komarov AP, Komarova EA, Green K, et al. Functional genetics-directed identification of novel pharmacological inhibitors of FAS- and TNF-dependent apoptosis that protect mice from acute liver failure. *Cell Death Dis*. 2016;7:e2145.

148. Yasuda M, Tanaka Y, Ryu M, Tsuda S, Nakazawa T. RNA sequence reveals mouse retinal transcriptome changes early after axonal injury. *PLoS One*. 2014;9:e93258.

149. Silverman SM, Kim BJ, Howell GR, et al. C1q propagates microglial activation and neurodegeneration in the visual axis following retinal ischemia/reperfusion injury. *Mol Neurodegener*. 2016;11:24.

150. Yin M, Tian S, Huang X, Huang Y, Jiang M. Role and mechanism of tissue plasminogen activator in venous wall fibrosis remodeling after deep venous thrombosis via the glycogen synthase kinase-3 beta signaling pathway. *J Surg Res*. 2013;184:1182–1195.

151. Collinge JE, Simirskii VN, Duncan MK. Expression of tissue plasminogen activator during eye development. *Exp Eye Res*. 2005;81:90–96.

152. Fernandes-Freitas I, Owen BM. Metabolic roles of endocrine fibroblast growth factors. *Curr Opin Pharmacol*. 2015;25: 30–35.

153. Uriarte I, Latasa MU, Carotti S, et al. Ileal FGF15 contributes to fibrosis-associated hepatocellular carcinoma development. *Int J Cancer*. 2015;136:2469–2475.

154. Grote K, Bavendiek U, Grothusen C, et al. Stretch-inducible expression of the angiogenic factor CCN1 in vascular smooth muscle cells is mediated by Egr-1. *J Biol Chem*. 2004;279:55675–55681.

155. Zhao W, Zhao J, Wang D, Li J. Screening of potential target genes for cataract by analyzing mRNA expression profile of mouse Hsf4-null lens. *BMC Ophthalmol*. 2015;15:76.

156. Liu Y, Zhou YD, Xiao YL, et al. Cyr61/CCN1 overexpression induces epithelial-mesenchymal transition leading to laryngeal tumor invasion and metastasis and poor prognosis. *Asian Pac J Cancer Prev*. 2015;16:2659–2664.

157. Hou CH, Lin FL, Hou SM, Liu JF. Cyr61 promotes epithelial-mesenchymal transition and tumor metastasis of osteosarcoma by Raf-1/MEK/ERK/Elk-1/TWIST-1 signaling pathway. *Mol Cancer*. 2014;13:236.

158. Meng Q, Lux A, Holloschi A, et al. Identification of Tctex2beta, a novel dynein light chain family member that interacts with different transforming growth factor-beta receptors. *J Biol Chem*. 2006;281:37069–37080.

159. Sachdev P, Menon S, Kastner DB, et al. G protein beta gamma subunit interaction with the dynein light-chain component Tctex-1 regulates neurite outgrowth. *EMBO J*. 2007;26: 2621–2632.

160. Béguin PC, Gosselin H, Mamarbachi M, Calderone A. Nestin expression is lost in ventricular fibroblasts during postnatal development of the rat heart and re-expressed in scar myofibroblasts. *J Cell Physiol*. 2012;227:813–820.

161. Chabot A, Hertig V, Boscher E, et al. Endothelial and epithelial cell transition to a mesenchymal phenotype was

delineated by nestin expression. *J Cell Physiol*. 2016;231: 1601–1610.

162. Rani SG, Sepuru KM, Yu C. Interaction of S100A13 with C2 domain of receptor for advanced glycation end products (RAGE). *Biochim Biophys Acta*. 2014;1844:1718–1728.

163. Huang S, Liu F, Niu Q, et al. GLIPR-2 overexpression in HK-2 cells promotes cell EMT and migration through ERK1/2 activation. *PLoS One*. 2013;8:e58574.

164. Ma L, Cantrup R, Varrault A, et al. Zac1 functions through TGFbetaII to negatively regulate cell number in the developing retina. *Neural Dev*. 2007;2:11.

165. Kosla J, Dvorakova M, Dvorak M, Cermak V. Effective myofibroblast dedifferentiation by concomitant inhibition of TGF-β signaling and perturbation of MAPK signaling. *Eur J Cell Biol*. 2013;92:363–373.

166. Kayam G, Kohl A, Magen Z, et al. A novel role for Pax6 in the segmental organization of the hindbrain. *Development*. 2013;140:2190–2202.

167. Munjal C, Opoka AM, Osinska H, James JF, Bressan GM, Hinton RB. TGF-β mediates early angiogenesis and latent fibrosis in an Emilin1-deficient mouse model of aortic valve disease. *Dis Model Mech*. 2014;7:987–996.

168. Iwazu Y, Muto S, Hirahara I, Fujisawa G, Takeda S, Kusano E. Matrix metalloproteinase 2 induces epithelial-mesenchymal transition in proximal tubules from the luminal side and progresses fibrosis in mineralocorticoid/salt-induced hypertensive rats. *J Hypertens*. 2011;29:2440–2453.

169. Han CY, Lim SW, Koo JH, Kim W, Kim SG. PHLDA3 overexpression in hepatocytes by endoplasmic reticulum stress via IRE1-Xbp1s pathway expedites liver injury. *Gut*. 2016;65:1377–1388.

170. Kawase T, Ohki R, Shibata T, et al. PH domain-only protein PHLDA3 is a p53-regulated repressor of Akt. *Cell*. 2009;136: 535–550.

171. Jeong K, Kwon H, Lee J, Jang D, Pak Y. Insulin-response epigenetic activation of Egr-1 and JunB genes at the nuclear periphery by A-type lamin-associated pY19-Caveolin-2 in the inner nuclear membrane. *Nucleic Acids Res*. 2015;43:3114–3127.

172. Hodge C, Liao J, Stofega M, Guan K, Carter-Su C, Schwartz J. Growth hormone stimulates phosphorylation and activation of elk-1 and expression of c-fos, egr-1, and junB through activation of extracellular signal-regulated kinases 1 and 2. *J Biol Chem*. 1998;273:31327–31336.

173. Gervasi M, Bianchi-Smiraglia A, Cummings M, et al. JunB contributes to Id2 repression and the epithelial-mesenchymal transition in response to transforming growth factor-β. *J Cell Biol*. 2012;196:589–603.

174. Gonen T, Grey AC, Jacobs MD, Donaldson PJ, Kistler J. MP20, the second most abundant lens membrane protein and

member of the tetraspanin superfamily, joins the list of ligands of galectin-3. *BMC Cell Biol*. 2001;2:17.

175. Casanegra AI, Stoner JA, Tafur AJ, Pereira HA, Rathbun SW, Gardner AW. Differences in galectin-3, a biomarker of fibrosis, between participants with peripheral artery disease and participants with normal ankle-brachial index. *Vasc Med*. 2016;21:437–444.

176. Vahedi S, Chueh FY, Chandran B, Yu CL. Lymphocyte-specific protein tyrosine kinase (Lck) interacts with CR6-interacting factor 1 (CRIF1) in mitochondria to repress oxidative phosphorylation. *BMC Cancer*. 2015;15:551.

177. Zheng X, Li Y, Zhao R, et al. xCT deficiency induces autophagy via endoplasmic reticulum stress activated p38-mitogen-activated protein kinase and mTOR in sut melanocytes. *Eur J Cell Biol*. 2016;95:175–181.

178. Evonuk KS, Baker BJ, Doyle RE, et al. Inhibition of system Xc(–) transporter attenuates autoimmune inflammatory demyelination. *J Immunol*. 2015;195:450–463.

179. Lewerenz J, Sato H, Albrecht P, et al. Mutation of ATF4 mediates resistance of neuronal cell lines against oxidative stress by inducing xCT expression. *Cell Death Differ*. 2012; 19:847–858.

180. Mandal PK, Seiler A, Perisic T, et al. System x(c)- and thioredoxin reductase 1 cooperatively rescue glutathione deficiency. *J Biol Chem*. 2010;285:22244–22253.

181. Shingu T, Bornstein P. Overlapping Egr-1 and Sp1 sites function in the regulation of transcription of the mouse thrombospondin 1 gene. *J Biol Chem*. 1994;269:32551–32557.

182. Bige N, Shweke N, Benhassine S, et al. Thrombospondin-1 plays a profibrotic and pro-inflammatory role during ureteric obstruction. *Kidney Int*. 2012;81:1226–1238.

183. Hiscott P, Paraoan L, Choudhary A, Ordonez JL, Al-Khaier A, Armstrong DJ. Thrombospondin 1, thrombospondin 2 and the eye. *Prog Retin Eye Res*. 2006;25:1–18.

184. Tang K, Cai Y, Joshi S, et al. Convergence of eicosanoid and integrin biology: 12-lipoxygenase seeks a partner. *Mol Cancer*. 2015;14:111.

185. Suzuki H, Kayama Y, Sakamoto M, et al. Arachidonate 12/15-lipoxygenase-induced inflammation and oxidative stress are involved in the development of diabetic cardiomyopathy. *Diabetes*. 2015;64:618–630.

186. Shinde V, Pitale PM, Howse W, Gorbatyuk O, Gorbatyuk M. Neuronatin is a stress-responsive protein of rod photoreceptors. *Neuroscience*. 2016;328:1–8.

187. Sharma J, Mukherjee D, Rao SN, et al. Neuronatin-mediated aberrant calcium signaling and endoplasmic reticulum stress underlie neuropathology in Lafora disease. *J Biol Chem*. 2013;288:9482–9490.

188. Jolma A, Yan J, Whitington T, et al. DNA-binding specificities of human transcription factors. *Cell*. 2013;152:327–339.